Study on MIMO-STBC Adaptive Array for Multi-User Communication Systems in Fast Fading channel

Supawan Annanab

The University of Electro-Communications
September 2008

Study on MIMO-STBC Adaptive Array for Multi-User Communication Systems in Fast Fading channel

by

Supawan Annanab

A dissertation submitted in Partial Fulfillment
of the Requirements
for the Degree of

DOCTOR OF ENGINEERING

at

The University of Electro-Communications
september 2008

Study on MIMO-STBC Adaptive Array for Multi-User Communication Systems in Fast Fading channel

APPROVED BY SUPERVISORY COMMITTEE

Chairperson	Professor YOSHIO KARASAWA
Member	Professor TAKESHI HASHIMOTO
Member	Professor NOBUO NAKAJIMA
Member	Professor YASUSHI YAMAO
Member	Assoc. Professor TAKEO FUJII

Study on MIMO-STBC Adaptive Array for Multi-User Communication Systems in Fast Fading channel

Supawan Annanab

Abstract

Wireless communication using multiple-input multiple-output (MIMO) systems impressively improves channel capacity and bit error rate (BER) performance. MIMO systems provide a number of advantages compared to a single antenna system. Average channel capacity of an MIMO system is approximately proportional to the number of array elements. Another way to use the system is to realize transmit diversity. Recently a simple transmit diversity scheme, or Space Time Block Coding (STBC), using two transmit antennas has been introduced by Alamouti (1998) and extensively studied in many publications in fading effect due to multipath time delay. However, there still exists a question on how to exploit STBC over fading effect due to Doppler spread. Effect on compensation scheme for Doppler spread in fast fading is considered in this thesis. Over a fast fading channel, the channel changes rapidly within a symbol period due to vehicle motion. In this case channel estimator does not work satisfactorily.

In this thesis, a new transmission scheme with adaptive beamforming receiver has been proposed for multiuser over Rayleigh fading to improve channel estimation reliability. In the case of synchronous multi-user transmission, pilot signals and information data are transmitted concurrently. Moreover, the beamforming using Recursive Least Squares (RLS) algorithms is adopted for the continuous tracking of fading environment. Simulation results show that this scheme can mitigate the effect of Doppler spread in high frequency and suppress co-channel interference up to $N-1$ users with N receive antennas.

The above scheme is next extended to asynchronous multi-user MIMO STBC with adaptive array under a fast fading channel. The extended scheme utilizes MIMO-STBC and an antenna array with a tapped delay line at the receiver. Each user employs two transmit antennas and transmits data using STBC. The proposed scheme transmits pilot signals and information data in different time slot alternately. A performance criterion for designing such scheme is derived under an assumption of fast fading condition. It shows that the proposed scheme can suppress co-channel interference (CCI) and Doppler spread effectively .

Finally, the improving performance of synchronous and asynchronous transmission multi-user scheme in STBC transmission is conducted and shown. The performance of all receiver structures developed in this dissertation is validated by computer simulations.

Study on MIMO-STBC Adaptive Array for Multi-User Communication Systems in Fast Fading channel

Supawan Annanab

Abstract

Wireless communication using multiple-input multiple-output (MIMO) systems impressively improves channel capacity and bit error rate (BER) performance. MIMO systems provide a number of advantages compared to a single antenna system. Average channel capacity of an MIMO system is approximately proportional to the number of array elements. Another way to use the system is to realize transmit diversity. Recently a simple transmit diversity scheme, or Space Time Block Coding (STBC), using two transmit antennas has been introduced by Alamouti (1998) and extensively studied in many publications in fading effect due to multipath time delay. However, there still exists a question on how to exploit STBC over fading effect due to Doppler spread. Effect on compensation scheme for Doppler spread in fast fading is considered in this thesis. Over a fast fading channel, the channel changes rapidly within a symbol period due to vehicle motion. In this case channel estimator does not work satisfactorily.

In this thesis, a new transmission scheme with adaptive beamforming receiver has been proposed for multiuser over Rayleigh fading to improve channel estimation reliability. In the case of synchronous multi-user transmission, pilot signals and information data are transmitted concurrently. Moreover, the beamforming using Recursive Least Squares (RLS) algorithms is adopted for the continuous tracking of fading environment. Simulation results show that this scheme can mitigate the effect of Doppler spread in high frequency and suppress co-channel interference up to $N-1$ users with N receive antennas.

The above scheme is next extended to asynchronous multi-user MIMO STBC with adaptive array under a fast fading channel. The extended scheme utilizes MIMO-STBC and an antenna array with a tapped delay line at the receiver. Each user employs two transmit antennas and transmits data using STBC. The proposed scheme transmits pilot signals and information data in different time slot alternately. A performance criterion for designing such scheme is derived under an assumption of fast fading condition. It shows that the proposed scheme can suppress co-channel interference (CCI) and Doppler spread effectively .

Finally, the improving performance of synchronous and asynchronous transmission multi-user scheme in STBC transmission is conducted and shown. The performance of all receiver structures developed in this dissertation is validated by computer simulations.

Acknowledgments

"If you are grateful, I [your lord] will add more (favors) unto you; but if you show ingratitude, truly My punishment is terrible indeed"(Quran 14:7)

I am happy to acknowledge the inspiration of Allah (SWT), who gave me the confidence to pursue this work to its conclusion. By Allah's will, aid and support, the completion of this work has become a reality.

I would like to thank the following for their assistance, support and friendship during the course of my doctoral studies.

First, I am indebted to Professor Yoshio Karasawa for his unselfish commitment of time, trusted conscientious advice, sound guidance, sincere efforts, constant support and encouragement. Not only provide education support, but also financial support as well as some advice on my living in Japan. He is a kindhearted person who genuinely desires to see all of his students succeeded. I am gratefully honored to have an opportunity to be under his supervision.

Second I want to thank Professor Takeshi Hashimoto, Professor Nobuo Nakajima, Professor Yasushi Yamao and Associate Professor Takeo Fujii, the committee members, for their constructive suggestions and comments on the dissertation. I would like to thank Japanese language teachers who educated me to be able to use Japanese language and live a pleasant time in Japan. Thanks are also due to Associate Professor Mikio Shiga for his help in proofreading and editing the Japanese language in this thesis.

I am indebted to Ministry of Education, Culture, Sport, Science and Technology (MEXT) of Japan for supporting me financially.

My special thanks are due to my father, mother, sister and two brothers for their continuous love, encouragement and patience. I was born and have been surrounded by funny, optimistic and generous persons whom my success is effected by. Most of all I would like to thank my parents to permit my sister to come and stay with me for one and a half year in Japan. Without them, this dissertation would never have been completed. I would like to thank my friends in laboratory, in university and outside university for their encouragement and corporative spirit and for nice time we spent together.

I am also owe a million of thanks to my host families (Masuda family, Morita family, Abe family), Mrs.Yasuyo Kusumi and Mrs.Akiko Kobayashi for their friendships, fun and caring which made me feel homey.

Finally, I must confess in all humility and sincerity that only I am responsible for the shortcoming for this thesis.

this dissertation is dedicated to
my father, Smith
my mother, Vilaiwan
my sister, Sutthawan
my brothers, Sathana and Satis
for their deep love
and help in many ways

Contents

List of Tables

List of Figures

List of Abbreviations

AA Adaptive Array

BER Bit Error Rate

BPSK Binary Phase Shift Keying

BWA Broadband Wireless Access

CCI Co-Channel Interference

CNR Carrier to Noise Ratio

CSI Channel State Information

DSTBC Differential Space Time Block Coding

i.i.d. independent and identically distributed

ITS Intelligent Transport System

IST Inter Symbol Interference

MIMO Multiple Input Multiple Output

MISO Multiple Input Single Output

ML Maximum Likelihood

MMSE Minumum Mean Square Error

MRC Maximal Receive Combining

MS Mobile Station

OSTBC Orthogonal Space Time Block Coding

PAM Pulse Amplitude Modulation

PSD Power Spectral Density

PSK Pulse Shift Keying

QAM Quadrature Amplitude Modulation

QPSK Quadrature Phase Shift Keying

RF Radion Frequency

RLS Recursive Least Square

SIMO Single Input Multiple Output

SISO Single Input Single Output

SMI Sample Matrix Inversion

SNR Signal to Noise Ratio

SVD Single Value Decomposition

STBC Space Time Block Coding

TDLAA Tapped Delay Line Adaptive Array

WSS Wide Sense Stationary

List of Mathematical Notations

General notations

s scalar s

$\boldsymbol{s}$ vector $\boldsymbol{s}$

$\boldsymbol{S}$ matrix $\boldsymbol{S}$

$\boldsymbol{S}_{M \times N}$ matrix $\boldsymbol{S}$ with M rows and N columns

$\mathbf{I}$ identity matrix $\mathbf{I}$

Mathematical operation

$(\cdot)^*$ complex conjugate

$(\cdot)^T$ vector or matrix transpose operation

$(\cdot)^H$ complex vector or matrix Hermitian operation

$(\cdot)^{-1}$ inverse matrix operation

$|\cdot|$ matrix determinant operation

$Re(\cdot)$ real part operation

Φ_{xx} Autocorrelation function of in-phase component x

$J_0(\cdot)$ Bessel function of the first kind nth order

$Q(\cdot)$ Gaussian Q-function

Chapter 1

Introduction

1.1 Context of Work

Mobile communication systems have explosively grown through three generations for last ten years. It is providing various types of services such as broadcast, multimedia video, email, and multimedia message. The need of higher data rate, broader bandwidth and higher capacity leads to the limitations and difficulties for system designing. Recently, the development is continuing to support the demand of higher technologies by deploying multiple antennas at the transmitters and receivers known as Multiple Input Multiple Output(MIMO) channel. MIMO channel is one major breakthrough for increasing information throughput and channel capacity in mobile communication. In general, ability of MIMO is fully exemplified in multipath-rich environments. Especially in indoor environment, the scattering is sufficiently rich to provide substantial link capacity increases. The average channel capacity of such system is approximately proportional to the number of array elements[1]. Another attractive feature of MIMO is the diversity advantage which realizes a reliable communication link having the diversity order of $N_t N_r$ where N_t and N_r are the number of array elements at transmitter side and receiver side respectively. Single-user MIMO in indoor channel such as [2] which shows how training affects the capacity of a fading channel. Morover, training based scheme for SISO and MIMO, which called pilot symbol assisted, [3]-[13] have been extensively investigated in many publications for single-user. However, there still an existing question on multi-user MIMO transmission scheme in fast fading.

Fast fading due to large Doppler spread is one of the most serious problems in outdoor mobile communication. Fast fading channel is the channel which changes its state rapidly within a time interval between adjacent symbols due to the motion of user equipment. Therefore channel estimator does not work satisfactorily for high speed vehicular at high frequency. The example for this application is intelligent transport system (ITS) such as road-to-vehicle communication or inter-vehicle communication whose type values of Doppler spread is fast fading environment and the effect of delay spread is negligible. However, the parameter values are not specific yet in the new service, thereby in this dissertation we employ $f_D T_s$ for Doppler spread expression.

Up to now, the research based on the problem of having reliable channel estimation in fast fading environment has been studied in [14] by proposing channel extrapolation techniques.

Although interpolation or extrapolation techniques can realize delay-less tracking in some case, we pursue another fast tracking scheme without extrapolation in this thesis.

In this thesis we consider a transmit diversity scheme in fast fading environment. Transmit diversity schemes have been more attractive and widely applied for reducing the effect of multipath fading. Some interesting methods of transmit diversity have been suggested [15]-[24]. For example, differential-Space-Time Block Coding (D-STBC) proposed in [16] is known as a single user case robust to fast fading and D-STBC MIMO system has been researched in [25]-[29]. Although, D-STBC exercises effectiveness in fast fading, the receiving system becomes complicated in multi-user cases.

Furthermore, the adaptive beamforming is devoted at the reception. In mid-1990s, the terms of "smart antennas" and "adaptive antennas" were introduced. During the process of signaling, the array antenna can be made adaptive and changes its transmission or reception characteristics when the radio environment changes.

Using an array of antenna elements to improve a wireless connection is an old technique used by Gulielmo Marconi in 1901 to increase the gain of the Atlantic transmissions of Morse codes[30]. He used four 61 meters high tower antennas arranged in a circular array in Poldu, England to transmit the Morse signal for the letter "S", over the distance 3425 km to Signal Hill in St.John, Newfoundland. Today, array antennas in wireless communication systems are used to improve performance in several ways, not just for range improvement. Systems with array antennas in commercial operation have been reported for GSM networks [31, 32], fixed broadband wireless access networks (BWA)[33] and 3G CDMA networks [34]. A numerous field trials with antenna arrays have also been reported, see[35]-[41] among others. An adaptive beamforming for STBC in [42] is initially introduced for multi-user application in quasi-static multipath channel. Multiuser STBC signals from co-channel users are led to an adaptive beamforming stage. Due to array antenna utilization, co-channel interference can be mitigated based on spatial adaptive signal processing.

Working further on the application of Multiple Input Multiple Output Space Time Block Coding Adaptive Array (MIMO STBC AA) into multi-user mobile communications over fast fading channels, not any other generalized configuration and performance result, was adequate for time selective fading (narrow band fast fading channels). A generalized configuration of Adaptive Array for MIMO STBC and, particular, for Doppler spread condition of the next generation wireless communications networks is thus important. We shall address this problem and propose efficient and flexible configurations of MIMO STBC AA for both synchronous and asynchronous transmission schemes in fast fading effect in this work.

The original contributions of our work is presented in the next section.

1.2 Original Contributions

Several contributions on the Synchronous and Asynchronous transmission scheme and its performance have been made in this work. Parts of these contributions have been published or submitted for publication. The following list summarized our main contributions within the scope of this work.

1. First describes a novel configuration for synchronous multi-user Multiple-Input Multiple-Output (MIMO) system in mobile communication over fast fading channels using STBC and adaptive array, given in Chapter 4. This work is published in the *IEICE Transaction of Communications, vol.E90-B, no.9, Sept.2007* and also presented at *2006 International Symposium on Antennas and Propagation(ISAP'06), Singapore, Nov.1-4, 2006.*

2. Second is the evaluation of Asynchronous MIMO STBC Adaptive Array Transmission Scheme for Multiuser over Fast Fading Channel, given in Chapter 5. The work is published in *IEICE Transaction of Communications,Vol.E91-B,No.08,pp.2666-2673,Aug. 2008.* and will be presented in *2008 IEEE 68th Vehicular Technology Conference (VTC2008-Fall), Calgary, Canada, Sept. 21-24 2008.*

1.3 Thesis Overview

The thesis contains 7 chapters and is organized as follows.

Chapter 2 explains the propagation theory. First, the basic concepts and small scale fading classification is presented. Then the characteristic of small scale fading channels are described in details. These characteristics will classify the type of multipath propagation and lead us to the scope of our interest which is fast fading. The fading model is also given in this chapter. In this thesis, the target model is Rayleigh fading model. This section describes how to create signal model and the its characteristic.

Chapter 3 gives the overview on space time signal processing. First, we provide the Multiple Input Multiple Output (MIMO) channel and its capacity over flat fading channels based on the case of channel state information(CSI) known at both ends and, the case of CSI unknown to the transmitter, but known at the receiver. Next is the explanation on diversity techniques and space time coding which is divided into space time block coding(STBC).

Chapter 4 investigates MIMO in fast fading with STBC. In order to overcome fast fading problem, the base station allows implementation of adaptive array using recursive least squares (RLS) algorithms while the mobile station employs STBC with two transmit antennas. The proposed scheme adopts simultaneous transmission of data and pilot signals reducing control error caused by delay of obtaining CSI. The simulation results show that the proposed scheme can mitigate the effect of Doppler spread in higher frequency and suppress co-channel interference up to $N-1$ users with using N receiving antennas.

Chapter 5 describes asynchronous multi-user MIMO system in mobile communication robust to fast fading environment. At the mobile station, two transmit antennas in each user applying STBC transmit signals asynchronously while the base station allows implementation of tapped delay line adaptive array (TDLAA). The proposed scheme transmits the pilot signal and information data in different time slot alternately. It is to show that our scheme can suppress co-channel interference (CCI) and defeat Doppler spread effectively.

Chapter 6 concludes the thesis and gives topics for future research.

Chapter 2

Propagation Theory

One of impairments inherently presented in every wireless communication system, which must be recognized and effectively mitigated for the system to function well, is fading. Fading itself has been studied and classified into a number of different types. In this chapter we present a detailed mathematical analysis and some useful models for capturing the effect of Doppler spread. In Sec.2.1, we discuss the types of fading as the behavior of the wireless channel with respect to the transmit signal. Then we describe the statistical of a flat fading received signal envelop called Rayleigh distribution in sec.2.2.

2.1 Multipath Propagation

2.1.1 Small Scale Propagation

Radio-wave propagation through wireless channels is a complicated phenomenon characterized by three basic mechanisms. They are reflection, diffraction, and scattering [43]:

- Reflection occurs when a propagation electromagnetic wave impinges on a smooth surface with very large dimension compared to the RF signal wavelength(λ).
- Diffraction occurs when radio path between the transmitter and receiver is obstructed by dense body with large dimensions compared to λ, causing secondary waves to be formed behind the obstructing body. Diffraction is a phenomenon that accounts for RF energy traveling from transmitter to receiver without a line-of-sight path between the two. It is often termed shadowing because the diffracted field can reach the receiver even when shadowed by an impenetrable obstruction.
- Scattering occurs when a radio wave impinges on either a large rough surface or any surface whose dimensions are on the order of λ or less, causing the reflected energy to spread out (scatter) in all directions. In an urban environment, typical signal obstructions that yield scattering are lampposts, street signs and foliage. A precise mathematical description systems analyses. However, considerable efforts have been devoted to the statical modeling and characterization of these different effects. The result is a range of

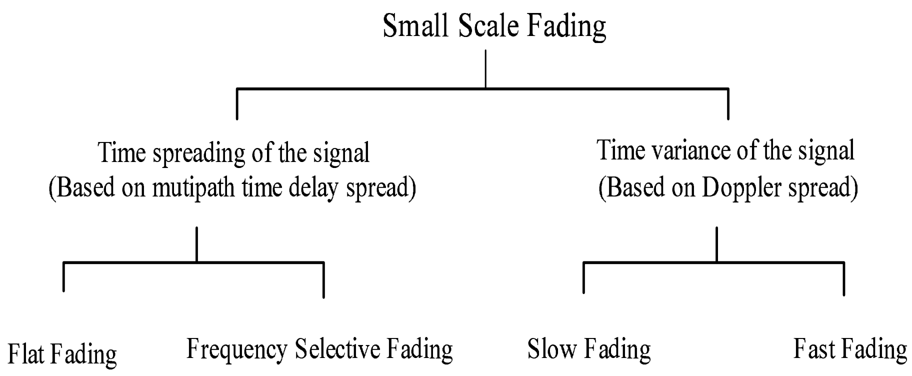

Figure 2.1: Small scale fading channel manifestations

relatively simple and accurate statistical models for fading channels which depend on the particular propagation environment and the underlying communication scenario.

When a received signal experiences fading during transmission, both its envelope and phase fluctuate over time. For coherent modulations, the phase fluctuations can severely degrade performance unless measures are taken to compensate for them at the receive. Most often, analyses of systems employing modulations assume that fluctuations are perfectly known at the receiver, resulting in what is referred to as coherent detection. For non-coherent detection, phase information is not needed at the receiver and therefore the phase fluctuations due to fading do not affect the performance analyses. Non-coherent detection over fading channels requires only knowledge of the fading envelop statistics. We will first review some basics of the fading channels. Figure 2.1 may serve as a table of contents for the sections that follow. We will examine the two manifestations of small scale fading: signal time-spreading (signal dispersion) and the time-variant nature of the channel.

2.1.2 Characteristic of Fading Channels

Fading radio channels have been classified in two ways. The first type of classification discusses whether the fading is flat (frequency non-selective) or frequency selective, while the second classification is based on the rate at which the channel is changing (or in other words, the rate of change of the impulse response of channel), i.e. whether the fading is slow or fast. In connection with these characterizations of fading channels, it is useful to note the following quantities:

Coherence bandwidth

Coherence bandwidth is a statistical measure of the range of frequencies over which the channel can be considered flat (i.e. frequency non-selective, or in other words a channel which passes all spectral components with equal gain and phase). It may also be defined as the range of frequencies over which any two frequency components have a strong potential for amplitude correlation. It has been shown that

$$B_c \propto \frac{1}{\sigma_\tau} \tag{2.1}$$

where σ_τ is the RMS delay spread. Also, if we define the coherence bandwidth as that bandwidth over which the frequency correlation function is above 0.9 then $B_c \approx \frac{1}{50\sigma_\tau}$. Note that if the signal bandwidth is more than Coherence bandwidth ($B_s > B_c$), then the different frequency components in the signal will not be faded the same way. The channel then appears to be frequency selective to the transmitted signal.

Doppler spread and Coherence time

While σ_τ and B_c describe the time dispersive nature of the channel in an area local to the receiver, they do not offer any information about the time-variations of the channel due to relative motion between the transmitter and their receiver. The Doppler spread B_D, defined as a measure of spectral broadening caused by the time-rate of change of the channel (related to the doppler frequency). The coherence time is a statistical measure of the time duration over which two received signals have a strong potential for amplitude correlation. Thus if the inverse bandwidth of the baseband signal is greater than the coherence time of the channel then the channel changes during transmission of the base band message. This will cause a distortion at the receiver. It is shown that

$$T_c \approx \frac{1}{f_D} \tag{2.2}$$

If the coherence time is defined as the duration of time over which the time correlation function is more than 0.5, then [43]

$$T_c \approx \frac{9}{16\pi f_D} \tag{2.3}$$

where f_D is the maximum Doppler frequency given by $f_D = v/\lambda$

Flat fading

If a channel has a constant response for a bandwidth more than the transmitted signal bandwidth, then the channel is said to be a flat fading channel. The conditions for a flat fading channel are

$$B_s \ll B_c \tag{2.4}$$

$$T_s \gg \sigma_\tau \tag{2.5}$$

where B_s and T_s are the signal bandwidth and the symbol duration respectively.

Frequency Selective Fading

A channel is said to be frequency selective if the signal bandwidth is greater than the coherence bandwidth of the channel. In such a case, different frequency components of the transmit signal undergo fading to different extents. For a frequency-selective fading situation

$$B_s \gtrsim B_c \tag{2.6}$$

$$T_s \lesssim \sigma_\tau \tag{2.7}$$

A common rule of thumb to characterize a channel as frequency selective is that if [43]

$$\sigma_\tau > 0.1 T_s \tag{2.8}$$

Slow Fading

In a slow fading channel, the channel impulse response changes at a rate much slower than the transmitted baseband signal $S(t)$. In the frequency domain, this implies that the Doppler spread of the channel is much less than the bandwidth of the baseband signal. Therefore, a signal undergoes slow fading if:

$$T_s \ll T_c \tag{2.9}$$

$$B_s \gg B_D \tag{2.10}$$

where B_D is the Doppler spread of the channel and T_c is its coherence time.

Fast Fading

In a fast fading channel, the channel impulse response changes rapidly within the symbol duration, i.e. the coherence time of the channel is smaller than the symbol period of the transmitted signal. Viewed in the frequency domain, signal distortion due to fast fading increases with increasing Doppler spread relative to the bandwidth of the transmitted signal. Therefore, a signal undergoes fast fading

$$T_s \gtrsim T_c \tag{2.11}$$

$$B_s \lesssim B_D \tag{2.12}$$

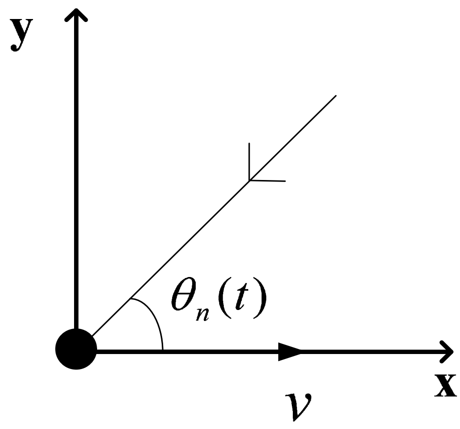

Figure 2.2: A mobile station moving along the positive x-axis at the velocity of v m/s for the n^{th} incoming wave at an angle of $\theta_n(t)$

2.2 Flat Rayleigh Fading Model[44, 45]

Figure 2.2 shows a mobile receiver (mobile station or MS) which is assumed to move along x axis with a velocity v m/s. The figure shows one of the many waves arriving at the mobile station. Let us call this the n^{th} incoming wave. Let it be incident at an angle $\theta_n(t)$, where the dependence on t stems from the fact that the receiver is not stationary.

The motion of MS produces a Doppler shift in the received frequency as compared to the carrier frequency. This Doppler offset is given by

$$f_{D,n}(t) = f_D \cos(\theta_n(t)) \tag{2.13}$$

where f_D (maximum Doppler frequency) $= v/\lambda$, λ being the wavelength of the radio wave. Waves arriving from the direction of motion cause a positive Doppler shift, while those coming from the opposite direction cause a negative Doppler shift. We wish to derive a mathematical framework to characterize the effects of small scale fading. Consider the transmit passband signal

$$s(t) = Re\{u(t)e^{j2\pi f_c t}\} \tag{2.14}$$

where $u(t)$ is the complex baseband equivalent to the passband transmit signal. If N waves arrive at the MS, the received passband signal can be written as

$$x(t) = Re\{r(t)e^{j2\pi f_c t}\} \tag{2.15}$$

with

$$r(t) = \sum_{n=1}^{N} \alpha_n(t)e^{-j2\pi\phi_n(t)}u(t - \tau_n(t)) \tag{2.16}$$

where multipath delay is τ_n, amplitude is α_n and

$$\phi_n(t) = (f_c + f_{D,n}(t))\tau_n - f_{D,n}(t)t \tag{2.17}$$

is the phase associated with the n^{th} wave. The above expression for $r(t)$ looks like the output of a linear time-varying system. Therefore the channel can be modeled as a linear filter with a time varying impulse response given by

$$c(\tau, t) = \sum_{n=1}^{N} \alpha_n(t) e^{-j\phi_n(t)} \delta(\tau - \tau_n(t)) \tag{2.18}$$

where $c(\tau, t)$ is the channel response at time t to an input at time $t - \tau$. The delays themselves are random. This implies that the phases of the incoming waves are random. The $\alpha_n(t)$'s are not very different from one another, i.e. the $\alpha_n(t)$'s do not change much over a small time scale. Therefore the received signal is a sum of a large number of waves with random phases. The random phases imply that sometime these waves add constructively producing a received signal with large amplitude, while at other times they add destructively, which low amplitude. This precise effect is termed small-scale fading, and the time scale at which the resulting fluctuation of amplitude occurs is the order of carrier frequency cycle wave. The range amplitude variation result can be up to 60 to 70 dB. Small scale fading is therefore primarily due to the random variations in phase $\phi_n(t)$ and also because of the Doppler frequency f_D. Flat fast fading condition, the consideration of delay is ignore, then we continue to express the modeling of received signal as

$$r(t) = \sum_{n=1}^{N} \alpha_n(t) e^{-j\phi_n(t)} \tag{2.19}$$

$$\begin{aligned} x(t) &= Re\{\sum_{n=1}^{N} \alpha_n(t) e^{-j\phi_n(t)} e^{j2\pi f_c t}\} \\ &= r_I(t)\cos(2\pi f_c t) - r_Q(t)\sin(2\pi f_c t) \end{aligned} \tag{2.20}$$

where

$$r_I(t) = \sum_{n=1}^{N} \alpha_n(t)\cos(\phi_n(t)) \tag{2.21}$$

$$r_Q(t) = -\sum_{n=1}^{N} \alpha_n(t)\sin(\phi_n(t)) \tag{2.22}$$

$$r(t) = r_I(t) + jr_Q(t) \tag{2.23}$$

$r_I(t)$ and $r_Q(t)$ are respectively the in-phase and the quadrature-phase components of the complex base-band equivalent of the received signal. Now we invoke the Central Limit theorem for large N. This makes $r_I(t)$ and $r_Q(t)$ independent Gaussian random processes. Further, assuming all the random processes are changing slowly enough to considered constant over the time intervals of interest, we have

$$f_{D,n}(t) = f_{D,n} \tag{2.24}$$

$$\alpha_n(t) = \alpha_n \tag{2.25}$$

$$\tau_n(t) = \tau_n \tag{2.26}$$

We assume that $x(t)$ is wide-sense stationary (WSS).

$$\begin{aligned} \Phi_{xx}(t) &= E\{x(t)x(t+\tau)\} \\ &= \Phi_{r_I r_I}(\tau)\cos(2\pi f_c t) - \Phi_{r_Q r_I}(\tau)\sin(2\pi f_c t) \end{aligned} \tag{2.27}$$

where,

$$\begin{aligned} \Phi_{r_I r_I}(\tau) &= E\{r_I(t) r_I(t+\tau)\} \\ &= E\{\{\sum_{i=1}^{N} \alpha_i \cos(\phi_i t)\}.\{\sum_{j=1}^{N} \alpha_j \cos(\phi_j (t+\tau))\}\} \end{aligned} \tag{2.28}$$

We can assume the ϕ_j 's are independent.

$$\phi_n(t) = \text{Uniformly distribution in}[-\pi, \pi] \tag{2.29}$$

On the evaluation of expectations, we get

$$\Phi_{r_I r_I}(\tau) = \frac{\Omega}{2} E\{\cos(2\pi f_{D,n} \tau)\} \tag{2.30}$$

where

$$\frac{\Omega}{2} = \frac{1}{2} \sum_{i=1}^{N} E\alpha_i^2 \tag{2.31}$$

is the total average received power from all multipath components. Now, in the expression above (2.30), we have

$$f_{D,n} = f_D \cos(\theta_n) \tag{2.32}$$

Therefore, we have the auto correlation function of the in-phase component $r_I(t)$

$$\Phi_{r_I r_I}(\tau) = \frac{\Omega}{2} E_\theta\{\cos(2\pi f_D \tau \cos(\theta_n))\} \tag{2.33}$$

Going through a similar series of steps for the cross-correlation function between the in-phase and quadrature phase component, we get

$$
\begin{aligned}
\Phi_{r_I r_Q}(\tau) &= E\{r_I(t) r_Q(t+\tau)\} \\
&= \frac{\Omega_p}{2} E_\theta\{\sin(2\pi f_D \tau \cos(\theta_n))\}
\end{aligned}
\tag{2.34}
$$

In order to simplify (2.33) and (2.34), we must make additional assumptions about the propagation environment. We will focus on the uniform scattering environment introduced by Clark [44] and further developed by Jakes [45]. In this model the channel consists of many scatterers densely packed with respect to angle (i.e. the incoming angle θ is uniformly distributed over $(-\pi, \pi)$). Then the above is called the Clarke's model. Using the uniform distribution for θ in the above, we get

$$
\Phi_{r_I r_I}(\tau) = \frac{\Omega}{2} \frac{1}{2\pi} \int_{-\pi}^{\pi} \cos(2\pi f_D \tau \cos(\theta)) d\theta \tag{2.35}
$$

which with a change of variable gives us

$$
\begin{aligned}
\Phi_{r_I r_I}(\tau) &= \frac{\Omega}{2} \frac{1}{\pi} \int_{0}^{+\pi} \cos(2\pi f_D \tau \sin(\theta)) d\theta \\
&= \frac{\Omega}{2} J_0(2\pi f_D \tau)
\end{aligned}
\tag{2.36}
$$

where $J_0(.)$ is the Bessel function of the zeroth order of the first kind. Similarly, using the uniform pdf for θ in the expression for cross correlation of the in-phase and quadrature phase component of $r(t)$ gives

$$
\Phi_{r_I r_Q} = 0 \tag{2.37}
$$

We are now in a position to talk about the power spectral density(PSD) of $r_I(t)$

$$
\begin{aligned}
S_{r_I r_I} &= \mathcal{F}[\Phi_{r_I r_I}(\tau)] \\
&= \begin{cases} \frac{\Omega}{4\pi f_D} \frac{1}{\sqrt{1-(\frac{f}{f_D})^2}} & |f| < f_D \\ 0 & \text{otherwise} \end{cases}
\end{aligned}
\tag{2.38}
$$

Having obtained the PSD of $r_I(t)$, we can now proceed to derive the PSD $x(t)$ as follows

$$
\Phi_{rr}(t) = E\{r^*(t).r(t+\tau)\} = \Phi_{r_I r_I}(\tau) + j\Phi_{r_I r_Q}(\tau) \tag{2.39}
$$

Therefore

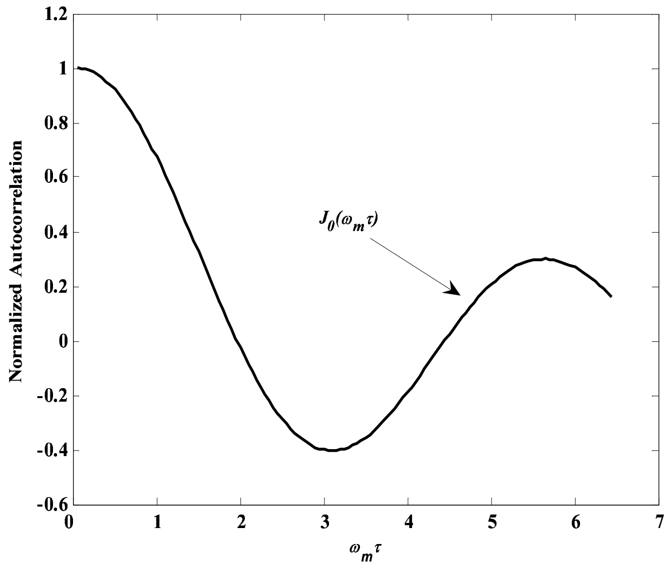

Figure 2.3: Bessel function of the zeroth order of the first type. This is the shape of the autocorrelation function $\Phi_{r_I r_I}(\tau)$ for the in-phase component of the complex baseband equivalent of the received signal

$$\Phi_{rr}(\tau) = \Phi_{r_I r_I}(\tau) \tag{2.40}$$

Further

$$\begin{aligned}\Phi_{xx}(\tau) &= Re\{\Phi_{rr}(\tau)e^{j2\pi f_c t}\} \\ &= Re\{\Phi_{r_I r_I}(\tau)e^{j2\pi f_c t}\}\end{aligned} \tag{2.41}$$

$$\begin{aligned}S_{xx}(f) &= \mathcal{F}\{Re\{\Phi_{r_I r_I}e^{j2\pi f_c t}\}\} \\ &= \mathcal{F}\{\frac{\Phi_{r_I r_I}(\tau)e^{j2\pi f_c t} + \Phi^*_{r_I r_I}(\tau)e^{-j2\pi f_c t}}{2}\}\end{aligned} \tag{2.42}$$

Note that $\Phi_{r_I r_I}(\tau) = \Phi^*_{r_I r_I}(-\tau)$, and so for real $r_I(t)$, $\Phi_{r_I r_I}(\tau) = \Phi_{r_I r_I}(-\tau)$ Thus we have

$$S_{xx}(f) = \mathcal{F}\{\frac{\Phi_{r_I r_I}(\tau)e^{j2\pi f_c t} + \Phi_{r_I r_I}(\tau)e^{-j2\pi f_c t}}{2}\} \tag{2.43}$$

$$S_{xx}(f) = \frac{1}{2}\{S_{r_I}S_{r_I}(f - f_c) + S_{r_I}S_{r_I}(-f - f_c)\} \tag{2.44}$$

Now we shall make use of the knowledge that the $r(t) = r_I(t) + jr_Q(t)$ is a complex Gaussian process for large N. Therefore the envelope $z(t) = |r(t)| = \sqrt{r_I^2(t) + r_Q^2(t)}$ has a Rayleigh distribution.

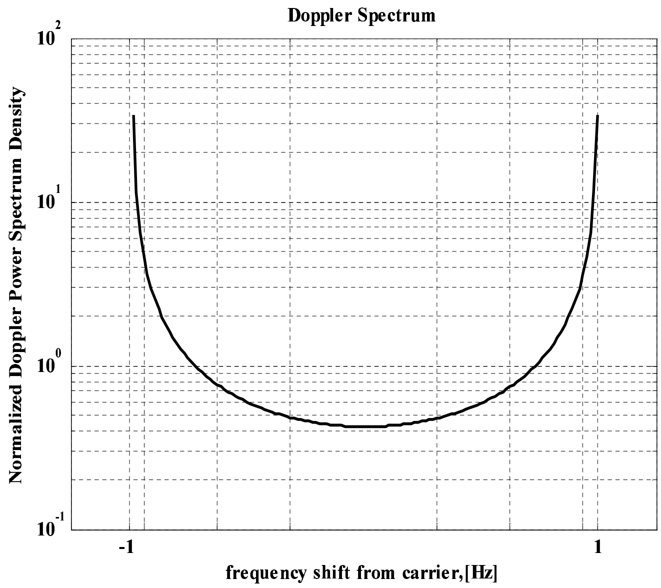

Figure 2.4: Power spectral density of the received signal, $S_{xx}(f)$
This is called the U-shaped PSD characteristic of Rayleigh fading modeled by the Jake's model

$$P_z(x) = \frac{x}{\sigma^2} \cdot e^{-x^2/2\sigma^2}; x \geqslant 0 \tag{2.45}$$

where $Ez^2 = \Omega_p = 2\sigma^2$ =average power. Thus we have the probability density function of the received signal given by

$$P_z(x) = \frac{x}{\Omega_p/2} . e^{-x^2/\Omega_p}; x \geqslant 0 \tag{2.46}$$

The above is called Rayleigh fading and is derived from Clarke's fading model, wherein the PSD of the received signal has the U-shape shown above. Rayleigh fading is generally applicable when there is no line-of-sight component. This is a good model for cellular mobile radio. Also note that the squared envelope $|r(t)|^2$ is exponentially distributed at any time

$$P_{z^2}(x) = \frac{1}{\Omega_p} e^{-x/\Omega_p}; x \geqslant 0 \tag{2.47}$$

Chapter 3

Overview of Space-Time Signaling

Schemes which use multiple transmit and receive antennas for communicating over a wireless channel are usually called Multiple-input multiple-output (MIMO) schemes. This chapter gives an introduction to MIMO systems or more specifically, space-time signaling; a technique used to transmit symbols from multiple antennas. This chapter is organized the performance of MIMO schemes. Moreover, explanation the concept of diversity, introduces transmit diversity[15]-[24],[46],[47] and provides a detailed description of the basic features of Space-Time Block Codes.

3.1 Multiple-Input Multiple-Output (MIMO) channels

To effectively evaluate the performance of a MIMO transmission scheme, models which account for all major effects of wireless channel on various signals are required. The most common used channel model for MIMO systems is quasi-static flat Rayleigh fading at all antenna elements. This is was employed in [20, 48]. The quasi-static flat Rayleigh fading MIMO channel for a system with N_t transmit and N_r receive antennas can be represented as

$$\boldsymbol{H} = \begin{bmatrix} h_{11} & h_{12} & \dots & h_{1N_t} \\ h_{21} & h_{22} & \dots & h_{2N_t} \\ \vdots & \vdots & \ddots & \vdots \\ h_{N_r1} & h_{N_r2} & \dots & h_{N_rN_t} \end{bmatrix} \tag{3.1}$$

where $h_{n_rn_t}$ is the path gain between receive antenna n_t and transmit antena n_r. We now define some concepts, begining with the MIMO signal model

$$\boldsymbol{r} = \boldsymbol{H}\boldsymbol{s} + \boldsymbol{n} \tag{3.2}$$

where $\boldsymbol{r}$ is the $N_r \times 1$ received signal vector, $\boldsymbol{s}$ is the $N_t \times 1$ transmitted signal vector and $\boldsymbol{n}$ is an $N_r \times 1$ vector of additive noise terms, assumed independent and identically distributed (i.i.d.) complex Gaussian with each element having a variance equal to σ^2. For convenience we normalize the noise power so that $\sigma^2 = 1$ in the remainder section.

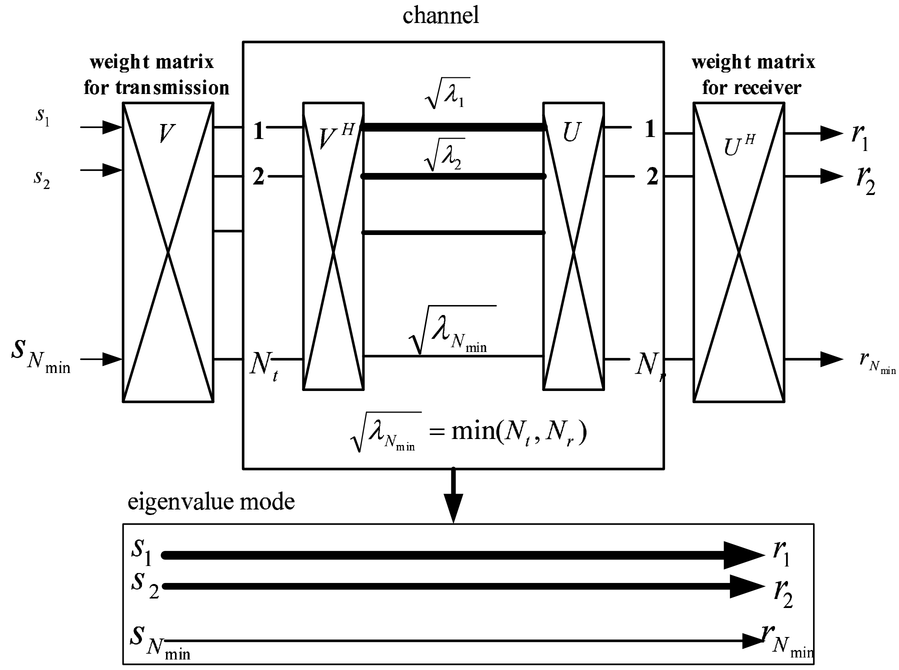

Figure 3.1: MIMO channel and Eigenvalue mode with N_{min} is the minimum antenna number between transmitter and receiver.

Channel Capacity of MIMO Flat Fading

For 1×1 (SISO) system the capacity is given by [49]

$$C = \log_2(1 + \rho|h|^2) \qquad \text{b/s/Hz} \tag{3.3}$$

where h is the normalized complex gain of a fixed wireless channel or that of a random channel and subsequently, ρ is the SNR at any receive antenna. As we deploy more receive antennas the statistics of capacity improve and with N_r receive antennas, we have a SIMO system with capacity given by

$$C = \log_2\left(1 + \rho \sum_{i=1}^{N_r} |h_i|^2\right) \qquad \text{b/s/Hz} \tag{3.4}$$

where h_i is the gain for receive antenna i. Similarly, if we adopt for transmit diversit, where the transmitter does not have channel knowledge, we have a multiple-input-single-output (MISO) system with N_t transmit antennas and the capacity is given by 3.3

$$C = \log_2\left(1 + \frac{\rho}{N_t} \sum_{i=1}^{N_t} |h_i|^2\right) \qquad \text{b/s/Hz} \tag{3.5}$$

where the normalization by N_t ensures a fixed total transmitter power and shows the absence of array gain in that case (compared to the case in 3.4, where the channel can be combined coherently). Now, we consider the use of diversity at both transmitter and receiver giving rise to MIMO system. For N_t transmitter and N_r receiver, we have the now famous capacity equation[56],[51],[52]

$$C_{EP} = \log_2 \left| \boldsymbol{I}_{N_r} + \frac{\rho}{N_t} \boldsymbol{H}\boldsymbol{H}^H \right| \qquad \text{b/s/Hz} \tag{3.6}$$

where $(.)^H$ means transpose-conjugate Note that both (3.5) and (3.6) are based on N_t equal power (EP) uncorrelated sources, hence, the capacity in (3.6) grows linearlity with $N_{min} = \min(N_r, N_t)$ rather than logarithmically. It is important to note that (3.6) can be rewritten as [51]

$$C_{EP} = \sum_{i=1}^{N_{min}} \log_2(1 + \frac{\rho}{N_t}\lambda_i) \qquad \text{b/s/Hz} \tag{3.7}$$

where $\lambda_1, \lambda_2, \cdots, \lambda_m$ are the nonzero eigenvalues of $\boldsymbol{H}^H\boldsymbol{H}$ and $\boldsymbol{H}\boldsymbol{H}^H$. This formulation can be easily obtained from the direct use of eigenvalue properties. Alternatively, we can decompose the MIMO channel into N_{min} equivalent parallel SISO channels be performing a singular value decomposition (SVD) of $\boldsymbol{H}$. Let the SVD be given by $\boldsymbol{H} = \boldsymbol{U}D\boldsymbol{V}^H$, the $\boldsymbol{U}$ and $\boldsymbol{V}$ are unitary matrix and D is diagonal matrix with entries specified by $D = diag(\sqrt{\lambda_1}, \sqrt{\lambda_2}, 0, \cdots, 0)$.

When the channel is known at the transmitter and at the receiver, then there is a simple algorithm to find the solution [51]-[55] called water filling (WF) optimization and the resulting capacity is given by

$$C_{WF} = \sum_{i=1}^{N_{min}} \log_2(\mu\lambda_i)^+ \qquad \text{b/s/Hz} \tag{3.8}$$

where μ is chosen to satisfy

$$\rho = \sum_{i=1}^{N_{min}} (\mu - \lambda_i^{-1})^+ \tag{3.9}$$

and "+"denotes taking only those terms which are positive.

3.2 Diversity Techniques and Space Time Coding

Let us consider a system with BPSK modulation transmitting under fading channel with Gaussian noise. The complex channel coefficient is denoted by h and its magnitude is denoted by α. It is assumed that the phase of fading coefficient is perfectly known at the receiver (i.e. coherent detection). The conditional error rate of BPSK as a function of channel coefficient over frequency non-selective, slowly fading channel is given by

$$P_b(\alpha) = Q(\sqrt{(2\gamma)}) \tag{3.10}$$

where $\gamma = \frac{\alpha^2 E_b}{N_0}$ is the received SNR and$Q(z) = \frac{1}{2}\text{erfc}(\sqrt{\gamma})$. To find unconditional error rate, we must integrate over all possible values of fading coefficient. Assuming Rayleigh fading, this integration is

$$P_b = \frac{1}{2}\left(1 - \sqrt{\frac{\bar{\gamma}}{1+\bar{\gamma}}}\right) \tag{3.11}$$

where $\bar{\gamma} = \frac{E_b}{N_0}\varepsilon(\alpha^2)$ is the average SNR. In high SNR region this error probability can be approximated as

$$P_b \approx \frac{1}{4\bar{\gamma}} \tag{3.12}$$

Note that the error rate decreases inversely with SNR. Compare this to the error rate of BPSK in non-fading (AWGN) channel

$$P_b = Q\left(\sqrt{\frac{2E_b}{N_0}}\right) \tag{3.13}$$

which decreases exponentially with SNR. This means that the transmitter should transmit with more power to achieve a low probability of error in a fading channel.

There are several types of diversity - frequency diversity, polarization diversity, time diversity and spatial diversity. In this thesis, we are only interested in spatial (antenna) diversity.

Traditionally, there is only single transmit antenna and multiple receive antenna. This technique is referred to as receive diversity. The receiver can use one of three techniques to improve the quality of received signal

1. Selection : select the received signal with largest received power.

2. Equal Gain Combining : The signals on each antenna combined by bringing all phase of the signals to a common reference point(cophasing). That is, the combined signal is the sum of the instantaneous fading envelopes of the individual brances.

3. Maximal Ratio Combining (MRC) : In maximum-ratio combining, the signal on each antenna is weighted by its instantaneous carrier-to-noise ration (CNR), refers to maximum CNR.

In the method of MRC, it is assumed that the receiver has perfect channel side information. If the transmitted signal at time t is $s(t)$, the received signal at receiver i is given by

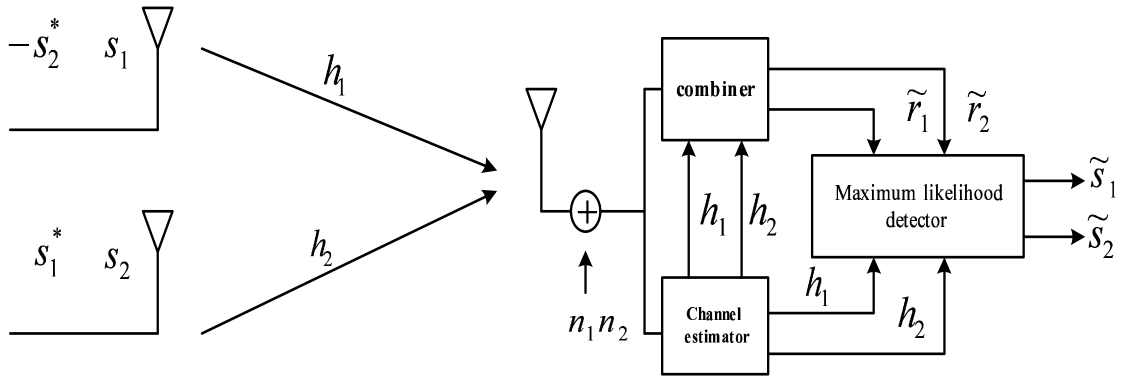

Figure 3.2: Space Time Block coding scheme with one receiver

$$r_i(t) = s(t)h_i(t) + n_i(t) \tag{3.14}$$

where $n_i(t)$ is complex noise variable. Assuming that this noise is Gaussian, the receiver combining scheme is

$$\begin{aligned} \tilde{r}(t) &= \sum_{i=1}^{N_r} h_i^* r_i(t) \\ &= s(t) \sum_{i}^{N_r} |h_i^2| + n^{'}(t) \end{aligned} \tag{3.15}$$

This detected symbol is then passed through a maximum-likelihood detector to produce the estimate of transmitted signal $\tilde{s}(t)$. MRC provides full diversity, but due to channel estimation the complexity is high.

Transmit Diversity and Space-Time Block Codes

The receive diversity scheme is not suitable for the downlink, as it is difficult and inconvenient to install multiple antennas on handsets. The multiple antenna burden is preferably placed at the base station. This is called transmit diversity. Transmit diversity has gained a lot of attraction and research in last ten years . Unlike in receive diversity, in transmit diversity it is not possible to transmit the same signal from all antennas. If same signal is transmitted from all the antennas, at the receiver the copies of this signal add incoherently, and no diversity gain can be achieved. Thus in order for transmit diversity to work, one must find a transmission scheme where replicas of the signal combine coherently at the receiver. One of the simplest and most attractive transmit diversity schemes were proposed by Alamouti [15],

$$\boldsymbol{G}_2 = \begin{pmatrix} s_1 & s_2 \\ -s_2^* & s_1^* \end{pmatrix} \tag{3.16}$$

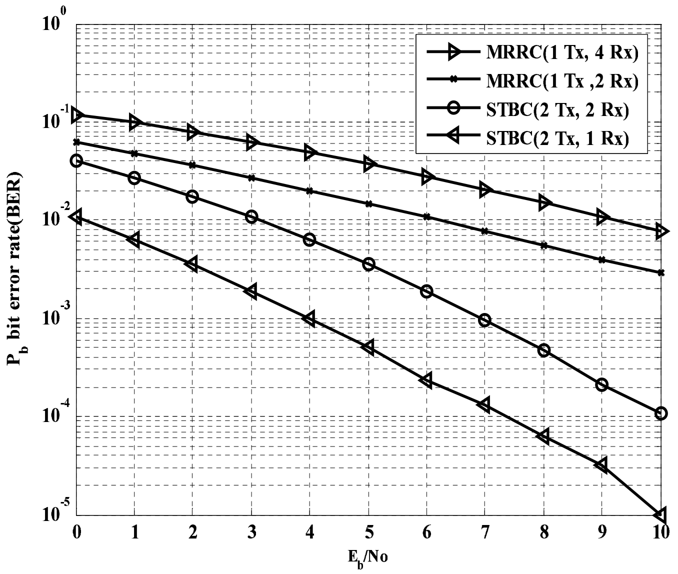

Figure 3.3: The BER performance comparison of BPSK with MRRC(Maximum Receive Ratio Combining)and Alamoti's scheme

where the rows denote time instances and columns denote transmit antennas. Thus, at time $t = 1$, s_1 and s_2 will be transmitted from antennas 1 and 2 respectively, and at time $t = 2$, $-s_2^*$ and s_1^* will be transmitted from antennas 1 and 2 respectively. One can see that two symbols are transmitted over two time intervals. Hence the code is full rate. Assuming a single receiver, let h_1 and h_2 denote the channel coefficients for transmit antenna 1 and 2 respectively. The fading coefficients are assumed to be constant over N_t = 2 consecutive time slots.

- $h_1 = h_1(T = 1) = h_1(T = 2)$
- $h_2 = h_2(T = 1) = h_2(T = 2)$

Hence the received signal is,

$$\begin{pmatrix} y_1 \\ y_2 \end{pmatrix} = \frac{1}{\sqrt{2}} \begin{pmatrix} s_1 & s_2 \\ -s_2^* & s_1^* \end{pmatrix} \begin{pmatrix} h_1 \\ h_2 \end{pmatrix} + \begin{pmatrix} n_1 \\ n_2 \end{pmatrix} \tag{3.17}$$

It can be rewritten as follows

$$\begin{pmatrix} y_1 \\ y_2^* \end{pmatrix} = \frac{1}{\sqrt{2}} \begin{pmatrix} h_1 & h_2 \\ -h_2^* & h_1^* \end{pmatrix} \begin{pmatrix} s_1 \\ s_2 \end{pmatrix} + \begin{pmatrix} n_1 \\ n_2^* \end{pmatrix} \tag{3.18}$$

$$\boldsymbol{y} = \frac{1}{\sqrt{2}} \boldsymbol{H}_e \boldsymbol{s} + \boldsymbol{n} \tag{3.19}$$

With perfect CSI, this can be maximum-likelihood (ML) decoded as,

$$\boldsymbol{r} = \boldsymbol{H}_e^H \boldsymbol{y} = \frac{1}{\sqrt{2}}(|h_1|^2 + |h_2|^2)\boldsymbol{s} + \boldsymbol{H}_e^H \boldsymbol{n} \tag{3.20}$$

We observe from the above expression that by using two transmit and one receive antenna, the transmitted signals are effectively multiplied by $|h_1|^2 + |h_2|^2$. Hence, if one of the paths is in deep fade, the other may still represent the signal with reliably. In fact, the use of orthogonal STBC changes the probability distribution of the channel to distribution with lower variance.

Tarokh et al. [16] extended the Alamouti's 2-transmit diversity scheme to more than two antennas. This new generalized space-time signaling scheme is known as space-time block codes (STBC). Space-time block codes derive their name from the fact that the encoding is done in both space and time, and their encoder is defined simply by a matrix. A space-time block code is defined by the relationship between the k-tuple input signal x and the set of signals to be transmitted from N_t antenna over p time periods. Such a relation is given by $p \times N_t$ transmission matrix

$$\boldsymbol{G} = \begin{bmatrix} s_{11} & s_{12} & \cdots & s_{1N_t} \\ s_{21} & s_{22} & \cdots & s_{2N_t} \\ \vdots & \vdots & \ddots & \vdots \\ s_{p1} & s_{p2} & \cdots & s_{pN_t} \end{bmatrix} \tag{3.21}$$

where s_{ij} are functions of k-tuple input sequence $x_1, x_2, ..., x_k$ and their complex conjugates. At time slot i, s_{ij} is transmitted from antenna j. Since k information bits are transmitted over p time interval, the rate of the code is defined as $R = \frac{k}{p}$ At the receiver we can use arbitrary number of receive antennas. The design does not depend on the number of receive antennas N_r. If $\boldsymbol{G}\boldsymbol{G}^H = \alpha I$ where $\alpha = \sum_{n=1}^{M} |s_n|$ and $\boldsymbol{I}$ is the identity matrix, the code is called orthogonal STBC. The other example of space time block coding constructions are

$$\boldsymbol{G}_3 = \begin{bmatrix} s_1 & s_2 & s_3 \\ -s_2 & s_1 & -s_4 \\ -s_3 & s_4 & s_1 \\ -s_4 & -s_3 & s_2 \\ s_1^* & s_2^* & s_3^* \\ -s_2^* & s_1^* & -s_4^* \\ -s_3^* & s_4^* & s_1^* \\ -s_4^* & -s_3^* & s_2^* \end{bmatrix} \tag{3.22}$$

From the above equation, With 3 transmit antennas $(N_t = 3)$ 4 types of data $(k = 4)$ and 8 time slots $(p = 8)$, the rate of the code is $1/2$.

$$
\boldsymbol{G}_4 = \begin{bmatrix} s_1 & s_2 & s_3 & s_4 \\ -s_2 & s_1 & -s_4 & s_3 \\ -s_3 & s_4 & s_1 & -s_2 \\ -s_4 & -s_3 & s_2 & s_1 \\ s_1^* & s_2^* & s_3^* & s_4^* \\ -s_2^* & s_1^* & -s_4^* & s_3^* \\ -s_3^* & s_4^* & s_1^* & -s_2^* \\ -s_4^* & -s_3^* & s_2^* & s_1^* \end{bmatrix} \tag{3.23}
$$

From the above equation, With 4 transmit antennas $(N_t = 4)$ 4 types of data $(k = 4)$ and 8 time slots $(p = 8)$, the rate of the code is $1/2$.

$$
\boldsymbol{H}_3 = \begin{bmatrix} s_1 & s_2 & \frac{s_3}{\sqrt{2}} \\ -s_2^* & s_1^* & \frac{s_3}{\sqrt{2}} \\ \frac{s_3^*}{\sqrt{2}} & \frac{-s_3^*}{\sqrt{2}} & (\frac{-s_1-s_1^*+s_2-s_2^*}{2} \\ \frac{-s_3^*}{\sqrt{2}} & \frac{-s_3^*}{\sqrt{2}} & \frac{(s_2+s_2^*+s_1-s_1^*)}{2} \end{bmatrix} \tag{3.24}
$$

From the above equation, With 3 transmit antennas $(N_t = 3)$ 3 types of data $(k = 3)$ and 4 time slots $(p = 4)$, the rate of the code is $3/4$.

$$
\boldsymbol{H}_4 = \begin{bmatrix} s_1 & s_2 & \frac{s_3}{\sqrt{2}} & \frac{s_3}{\sqrt{2}} \\ -s_2^* & s_1^* & \frac{s_3}{\sqrt{2}} & -\frac{s_3}{\sqrt{2}} \\ \frac{s_3^*}{\sqrt{2}} & \frac{-s_3^*}{\sqrt{2}} & (\frac{-s_1-s_1^*+s_2-s_2^*}{2} & (\frac{-s_2-s_2^*+s_2-s_1^*}{1} \\ \frac{-s_3^*}{\sqrt{2}} & \frac{-s_3^*}{\sqrt{2}} & \frac{(s_2+s_2^*+s_1-s_1^*)}{2} & \frac{(s_1+s_1^*+s_2-s_2^*)}{2} \end{bmatrix} \tag{3.25}
$$

From the above equation, With 3 transmit antennas $(N_t = 3)$ 3 types of data $(k = 3)$ and 4 time slots $(p = 4)$, the rate of the code is $3/4$. It can be verified that the columns of these matrices meet the orthogonality requirement. These codes have a simple linear processing rule, followed by a maximum likelihood decoder. As an example, the decoder for G_3 minimizes the following decision metrics

$$
\left| \left[\ \sum_{j=1}^{N} (|r_1^j \alpha_{1,j}^* + (r_2^j)\alpha_{2,j}^* + r_3^j \alpha_{3,j}^* + (r_5^j)^* \alpha_{1,j} + (r_6^j)^* \alpha_{2,j} + (r_7^j)^* \alpha_{3,j} \ \right] - s_1 \right|^2 \\ + \left(\ -1 + \sum_{j=1}^{N} \sum_{i=1}^{3} |\alpha_{i,j}^2| \ \right) |s_1|^2 \tag{3.26}
$$

for decoding s_1, and,

$$
\left| \left[\ \sum_{j=1}^{N} (|r_1^j \alpha_{2,j}^* - (r_2^j)\alpha_{1,j}^* + r_4^j \alpha_{3,j}^* + (r_5^j)^* \alpha_{2,j} - (r_6^j)^* \alpha_{1,j} + (r_8^j)^* \alpha_{3,j} \ \right] - s_2 \right|^2 \\ + \left(\ -1 + \sum_{j=1}^{N} \sum_{i=1}^{3} |\alpha_{i,j}^2| \ \right) |s_2|^2 \tag{3.27}
$$

for decoding s_2, and,

$$\Big|\Big[\ \sum_{j=1}^{N}(|r_1^j\alpha_{3,j}^* - (r_3^j)\alpha_{1,j}^* - r_4^j\alpha_{2,j}^* + (r_5^j)^*\alpha_{3,j} - (r_7^j)^*\alpha_{1,j} - (r_8^j)^*\alpha_{2,j}\ \Big] - s_3\Big|^2 + \Big(\ -1 + \sum_{j=1}^{N}\sum_{i=1}^{3}|\alpha_{i,j}^2|\ \Big)|s_3|^2 \quad (3.28)$$

for decoding s_3, and,

$$\Big|\Big[\ \sum_{j=1}^{N}(| - r_2^j\alpha_{3,j}^* + (r_3^j)\alpha_{2,j}^* - r_4^j\alpha_{1,j}^* - (r_6^j)^*\alpha_{3,j} + (r_7^j)^*\alpha_{2,j} - (r_8^j)^*\alpha_{1,j}\ \Big] - s_3\Big|^2 + \Big(\ -1 + \sum_{j=1}^{N}\sum_{i=1}^{3}|\alpha_{i,j}^2|\ \Big)|s_4|^2 \quad (3.29)$$

for decoding s_4.

The orthogonal STBC(OSTBC) assumes that the channel coefficients are constant over a period of N_t symbols, i.e.

$$h(t)_{ij} = h_{ij} \quad ; t = 1, 2, ..., N_t \quad (3.30)$$

This block fading assumption is required for simple linear decoding of OSTBC. OSTBC also assumes that the channel is frequency non-selective. At the receiver, the N_r receive antennas use maximum likelihood (ML) decoding. In orthogonal STBC the ML decoding is equivalent to maximum ratio combining (MRC). Assuming perfect channel State Information (CSI), the decoder at antenna j maximizes

$$\sum_{t=1}^{p}\sum_{j=1}^{N}|r_t^j - \sum_{i=1}^{M}h_{ji}x_t^i|^2 \quad (3.31)$$

Since the block coding requires only linear processing at the receiver, the decoding can be done efficiently and quickly. Space-time block codes can be constructed for any type of signal constellation and provide full diversity. However, only real constellations such as Pulse Amplitude Modulation(PAM) can give full rate for any number of antennas. For complex constellations such as Quadrature Phase Shift Keying (QPSK), full rate STBC exist only for $N_t = 2$.

Chapter 4

Synchronous Multi-user MIMO STBC Transmission Scheme in Fast Fading Environment

4.1 Introduction

We propose a simple STBC scheme [15] with device transmitting sequence of pilot signal and information data. Moreover, a novel channel tracking method is introduced in our system. The idea of this method is to transmit information data and pilot signal simultaneously through different antennas. Furthermore, introducing a reception with adaptive beamforming is a countermeasure for fast fading.

Spatio-temporal equalization for STBC in [42] is initially introduced for multi-user application in quasi-static multipath channel. Multiuser STBC signals from co-channel users are led to spatio-temporal processing which uses MMSE criterion and sample matrix inversion (SMI) algorithm. Due to array antenna utilization, co-channel interference can be mitigated based on spatial adaptive signal processing [58],[66].

In our scheme, the pilot signal and information data are transmitted simultaneously and then multiuser STBC signals from co-channel users will be proceeded. The beamforming can be done using Recursive Least Squares (RLS) algorithms for the continuous tracking of fast fading channel. The RLS algorithm in our applied case adapts only one of two weight vectors and hence the other weight vector can be computed based on the value of adapted weight vector. This is particularly useful as it overcomes large Doppler spread in high frequency and high speed conditions. Simulation results show that co-channel interference of up to $(N-1)$ users can be suppressed while applying N receiving antennas.

4.2 Channel Estimation

Channel estimation is the process of characterizing or analyzing the effect of the physical medium on the input sequence (transmitted data). The importance of channel estimation is

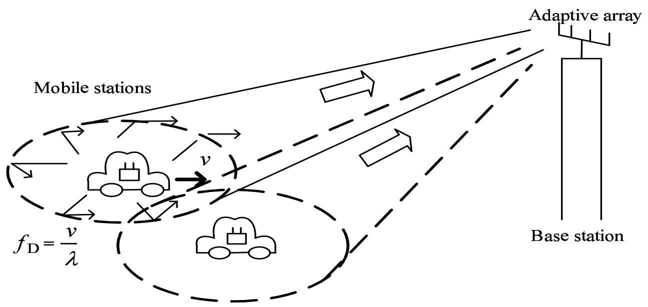

Figure 4.1: MIMO system for multi user mobile communication

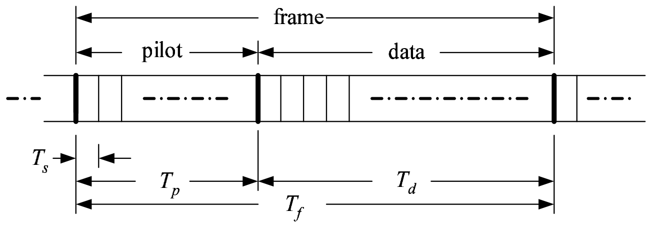

Figure 4.2: Conventional transmission signal sequence for adaptive array system

that it allows the receiver to take into account the effect of channel and to predict the transmitted signal for removing interference and noise. Since the system studied in this chapter is that in a very rapid time-varying fading, high speed estimation of the channel is essential.

There are two main types of channel estimation methods, namely blind methods and training sequence methods. In the blind method, mathematical or statistical properties of transmitted data are used. This makes the method extremely computationally intensive and thus hard to implement in real time systems. In training sequence methods, the transmitted data and training sequences known to the receiver are embedded into the frame and sent through the channel.

Training sequence method makes use of the training bits (pilot symbols) known to the receiver and is computationally simple compared to blind method. Insertion and extraction of pilot symbol enable to derivation the channel information and determination of array weights for data transmission. The transmitter periodically transmits known symbols, from which the receiver construct an estimate of the channel for every transmitted data symbol.

Performance of pilot insertion and extraction techniques are degraded by many factors, such as time variance of the channel. In the case of fast fading environment, the channel is assumed to be dynamic and is likely to change within the pilot symbols period. This leads to the demand of a transmitting method robust to time variation and error elimination at the receiver.

Table 4.1: Fast fading index β_0 for $v = 30m/s$ (or $108km/h$)

T_s \ f_c	2 GHz	5 GHz
1 μsec	0.0002	0.0005
10 μsec	0.002	0.005
100 μsec	0.02	0.05

4.2.1 Doppler Spread Effects

In order to evaluate the significance of Doppler effect in a system, we introduce fast fading index β_0 which is given by

$$\beta_0 = f_D T_s \tag{4.1}$$

Generally, transmitted signal with β_0 more than 0.01 [3, 4, 27] will be distorted by the effects of Doppler spread. A widely-used diagram of conventional transmission sequence for Adaptive Array (AA) is viewed in Fig. 4.2. Each frame T_f consists of pilot period T_p and data period T_d while symbol duration is assumed to be T_s.

In the case of adaptive array system with a pilot signal for antenna weight determination, transmission signal sequence shown in Fig.4.2 is necessary to keep a quasi-stationary condition during a period of T_f.

As long as effective fast fading index $\beta_e = f_D T_f$ is less than or equal to 0.01, the channel will not cause distortion by Doppler spread. Table 4.1 shows β_0 which can be estimated by assuming that the vehicular velocity is 30 m/s (108 km/h) at frequencies of 2 GHz and 5 GHz. Considering that β_e is usually 10 to 100 times larger than β_0, it can be noticed that a system in high frequency, high velocity and low symbol rate easily becomes fast fading condition.

4.2.2 Channel Model and Assumptions

We assume a narrowband fading channel which means that effect of delay spread is negligible while Doppler spread is considered. One application for this type of fading environment is road-to-vehicle communication or inter-vehicle communication in ITS, but not limited to this. In our simulation, we generate independent time-varying Rayleigh fading channel (i.i.d. Rayleigh fading channel) having the Jakes-type power spectrum [45] . Actually, we generate each fading channel based on Eq.(2.20) which can be explained in matrix form as the following equation

$$h_{n,m}^{(k)}(t)^1 = \frac{1}{\sqrt{I}} \sum_{i=1}^{I} e^{j(2\pi f_D cos\theta_i t + \phi_i)} \tag{4.2}$$

[1]Number of transmit antennas N_t is N and number of receive antennas N_r is M.

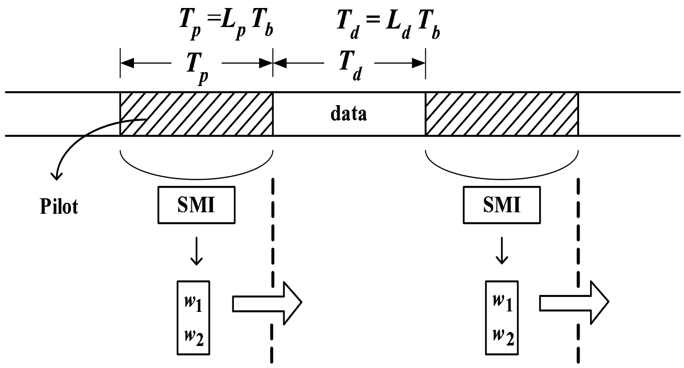

Figure 4.3: Conventional Transmitting method 1 for MIMO STBC AA

where θ_i is incident angle of path i and ϕ_i is initial phase, both of which are given by random number ranging from 0 to 2π. In order to realize accurate Rayleigh fading statistically, we set $I = 100$

4.3 Configuration and Signal Model

4.3.1 Conventional Method

For performance comparison of proposed method to conventional methods, we consider two methods, both of which transmit the pilot signal and information data in different time slot alternately. The conventional adaptive beamformings for STBC scheme are shown in Fig.4.3 [11] and 4.4 respectively. In method 1 (see Fig.4.3), each frame contains a minimal number of pilot symbols with a period of $T_p = L_p T_b$, where $T_b = 2T_s$, while mehod 2 (see Fig.4.4) with a period of T_b for weight determination and also in method 1, a number of data symbols with a period of $T_d = L_d T_b$ while method 2 with a period of LT_b. At the base station, a reception scheme with using an adaptive algorithm such as SMI (Sample Matrix Inversion) can be used for method 1 and RLS (Recursive Least Squares) for method 2. For these schemes, transmission symbol rate of method 1 and method 2 become $L_d \diagup (L_p + L_d)$ and $L \diagup (1 + L)$ times smaller than original data symbol rate. The rate reduction depends on the fast fading index for AA. In method 1, in order to work well in fast fading condition, values of L_p and L_d should be smaller as far as possible. However, if the value is too small (for example, less-than 10), the performance becomes degraded due to insufficient number of data during T_p (namely, an ill condition). Therefore we select Method 2 as a conventional method. In method 2, the transmission data rate decreases with decreasing L value, and its extreme is $L = 1$ which gives a half rate and is equal to our method.

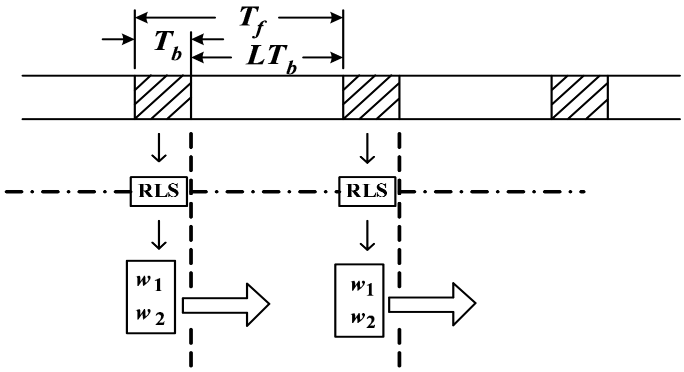

Figure 4.4: Conventional Transmitting method 2 for MIMO STBC AA

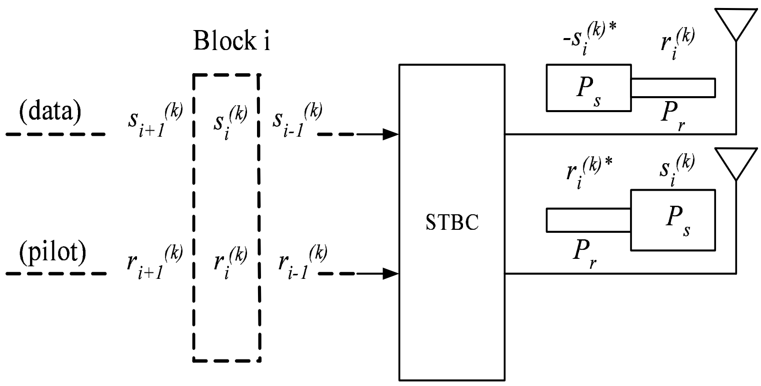

Figure 4.5: Proposed transmitting method

4.3.2 Proposed Scheme

MIMO STBC Adaptive Array scheme has been considered as a countermeasure for fast fading environment. Since delay of obtaining channel state information (CSI) causes significant control error of adaptive array in fast fading environment. For obtaining CSI, negligible delay is essential for the control. We adopt simultaneous transmission of data and pilot signals through different antennas.MIMO STBC Adaptive Array scheme has been considered as a countermeasure for fast fading environment. Since delay of obtaining channel state information (CSI) causes significant control error of adaptive array in fast fading environment. For obtaining CSI, negligible delay is essential for the control. We adopt simultaneous transmission of data and pilot signals through different antennas. The concept of this method is clarified in Fig4.5.

Concerning Block i for user k, data signal $s_i^{(k)}$ and pilot signal $r_i^{(k)}$ are transmitted at the same time. For the convenience of following discussions, let us define transmission power sharing between pilot signal and data signal as follows

$$P_r^{(k)} =< |r_i^{(k)}|^2 > \tag{4.3}$$

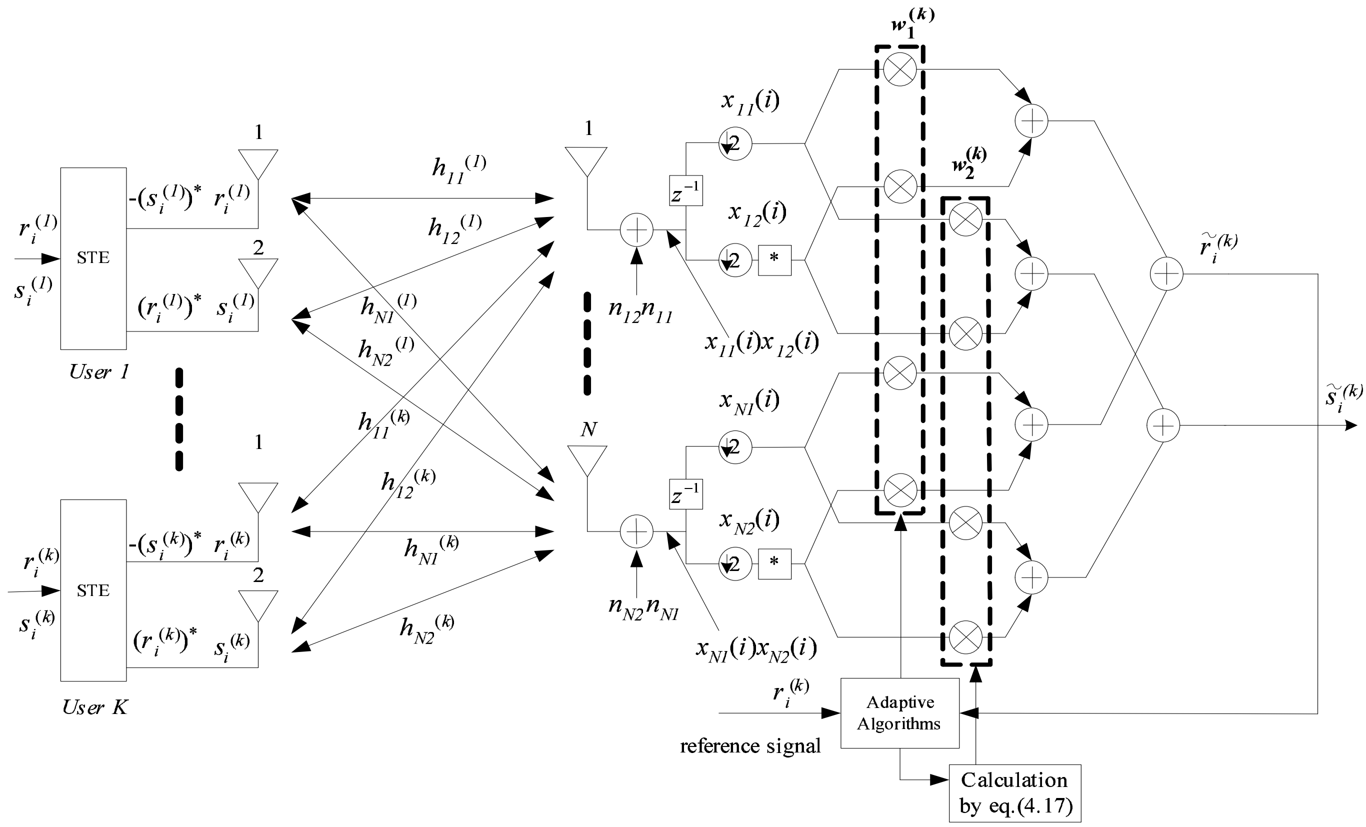

Figure 4.6: Adaptive Beamforming configuration for multiuser STBC (STE:Space Time Encoding)

$$P_s^{(k)} =< |s_i^{(k)}|^2 > \tag{4.4}$$

$$\xi^{(k)} = \frac{P_s^{(k)}}{P_s^{(k)} + P_r^{(k)}} \; ; \; P_r^{(k)} + P_s^{(k)} = const. \tag{4.5}$$

Where $< . >$ denotes ensemble average. The suitable value of power efficiency $\xi^{(k)}$ for all MSs will be dertermined later.

The proposed MIMO scheme employs STBC with AA at the base station as shown in Fig. 4.6. The scheme uses two transmit antennas in each user and N receive antennas. At transmission side, kth user at time t sends two symbols, pilot signal $r_i^{(k)}$ over its 1st antenna and transmission data $s_i^{(k)}$ over its 2nd transmit antenna. At the next symbol time, time $(t + T_s)$, where T_s is a symbol duration, antenna 1 transmits $-(s_i^{(k)})^*$ while antenna 2 transmits $(r_i^{(k)})^*$ where $(.)^*$ indicates the complex conjugate. This sequence is shown in Table4.2 [15].

On the other hand, the base station consists of reception processing and adaptive beamforming. In each receive antenna unit, the reception processing separates symbol into two streams

Table 4.2: The Encoding and Transmission sequence

	antenna 1	antenna 2
time t	$r_i^{(k)}$	$s_i^{(k)}$
time $t+T_s$	$-(s_i^{(k)})^*$	$(r_i^{(k)})^*$

namely odd stream (indexed as 1) for symbol transmitted at time t and even stream (indexed as 2) for symbol transmitted at time $t+T_s$. Note that it is necessary to take complex conjugate on the even stream, since all symbols transmitted at time $t+T_s$ are complex conjugated. After reception processing containing Additive White Gaussian Noise (AWGN) and other user signals, the signals from transmitted Block i in the nth receive antenna are given by

$$x_{n1}(i) = \sum_{k=1}^{K}[r_i^{(k)}h_{n1}^{(k)} + s_i^{(k)}h_{n2}^{(k)}] + n_{n1} \tag{4.6}$$

and

$$x_{n2}(i) = \sum_{k=1}^{K}[-(s_i^{(k)})^*h_{n1}^{(k)} + (r_i^{(k)})^*h_{n2}^{(k)}] + n_{n2} \tag{4.7}$$

Denote

$$\boldsymbol{x}_n(i) = \left[\begin{array}{cc} x_{n1}(i) & x_{n2}^*(i) \end{array}\right]^T \tag{4.8}$$

and define reception signal vector for Block i transmitted signal as

$$\boldsymbol{x}(i) = \left[\begin{array}{cccc} (\boldsymbol{x}_1(i))^T & (\boldsymbol{x}_2(i))^T & \dots & (\boldsymbol{x}_N(i))^T \end{array}\right]^T \tag{4.9}$$

where $(.)^T$ indicates vector transpose. The reception signal vector $\boldsymbol{x}(i)$ and $[2N \times 1]$ weight vector $\boldsymbol{w}_1^{(k)}$ are then combined to produce estimated pilot output $\tilde{r}_i^{(k)}$ and data output $\tilde{s}_i^{(k)}$. They are given by

$$\boldsymbol{w}_1^{(k)} = \left[\begin{array}{cccccc} w_{11}^{(k)} & w_{12}^{(k)} & \dots & w_{N1}^{(k)} & w_{N2}^{(k)} \end{array}\right]^T \tag{4.10}$$

$$\tilde{r}_i^{(k)} = (\boldsymbol{w}_1^{(k)})^H\boldsymbol{x}(i) \tag{4.11}$$

$$\tilde{s}_i^{(k)} = (\boldsymbol{w}_2^{(k)})^H\boldsymbol{x}(i) \tag{4.12}$$

where $(.)^H$ is the complex conjugate transpose. The optimal weights are chosen to minimize the mean-square error (MSE) between beamformer output and the reference signal such that

$$\boldsymbol{w}_{1_{opt}}^{(k)} = \arg\min < |r_i^{(k)} - (\boldsymbol{w}_1^{(k)})^H \boldsymbol{x}(i)|^2 > \tag{4.13}$$

The optimal weight $\boldsymbol{w}_{1_{opt}}^{(k)}(i)$ is time-variant and referred to optimum Wiener solution.

$$\boldsymbol{w}_1^{(k)}(i) = \boldsymbol{R}^{-1}(i)\boldsymbol{b}^{(k)}(i) \tag{4.14}$$

$$\boldsymbol{R}(i) = \gamma \boldsymbol{R}(i-1) + \boldsymbol{x}(i)\boldsymbol{x}^H(i) \tag{4.15}$$

$$\boldsymbol{b}^{(k)}(i) = \gamma \boldsymbol{b}^{(k)}(i-1) + (r_i^{(k)})^* \boldsymbol{x}(i) \tag{4.16}$$

where $\boldsymbol{R}$ is usually referred to as the covariance matrix or correlation matrix. In this chapter, we adopt Recursive Least Squares algorithm (RLS) to obtain weight vector $\boldsymbol{w}_1^{(k)}$. The forgetting factor $0 < \gamma < 1$ is a parameter of the RLS algorithms, and intends to follow temporal variation of CSI.

The weight vector $\boldsymbol{w}_2^{(k)}$ is determined directly from the obtained weight vector $\boldsymbol{w}_1^{(k)}$ (see Appendix A) as

$$\boldsymbol{w}_2^{(k)} = \begin{bmatrix} (w_{12}^{(k)})^* & -(w_{11}^{(k)})^* & \ldots & (w_{N2}^{(k)})^* & -(w_{N1}^{(k)})^* \end{bmatrix}^T \tag{4.17}$$

The time varying channel characteristic $H^{(k)}(t)$ for user k can be written in matrix form as

$$H^{(k)}(t) = \begin{bmatrix} h_{1,1}^{(k)}(t) & h_{1,2}^{(k)}(t) \\ \vdots & \vdots \\ h_{N,1}^{(k)}(t) & h_{N,2}^{(k)}(t) \end{bmatrix} \tag{4.18}$$

Denote the channel amplitude between a transmit antenna m of user k and a receive antenna n is a complex number $h_{n,m}^{(k)}(t)$ $(m = 1, 2; n = 1, \ldots, N)$ and the average channel power gain is set to 1 as follows

$$< |h_{11}^{(k)}|^2 > = < |h_{12}^{(k)}|^2 > = \ldots = < |h_{N2}^{(k)}|^2 > = 1 \tag{4.19}$$

Data signal power $P_s^{(k)}$ and pilot signal power $P_r^{(k)}$ are computed as in Eqs. 4.3 and 4.4, respectively. Summation of both power is called total power $P_t^{(k)}$, and is given by

$$P_t^{(k)} = P_s^{(k)} + P_r^{(k)} \tag{4.20}$$

Noise signals shown in Eqs. 4.6 and 4.7 can be explained in average power gain as follows

$$P_n = < |n_{11}|^2 > = < |n_{12}|^2 > = \ldots = < |n_{N2}|^2 > \tag{4.21}$$

The ratio of noise power P_n and total power $P_t^{(k)}$ intends to show $CNR^{(k)}$ calculation for the system as follows:

$$CNR^{(k)} = \frac{P_t^{(k)}}{P_n} \tag{4.22}$$

In this chapter, we assume that all of $CNR^{(k)}$ have the same value for k and simply denoted by CNR. The estimated $\tilde{r}_i^{(k)}$ and $\tilde{s}_i^{(k)}$ are then sent to Maximum Likelihood (ML) detector, which is not shown in Fig. 4.6, to make the decision rule for phase shift keying (PSK) signal.

4.4 Simulation and Results

Table 4.3 shows the simulation conditions for investigating performance of conventional and proposed MIMO STBC adaptive beamforming schemes. Each of 5 users evaluated here has two transmit antennas. Carrier to Noise Ratio (CNR) is set to be 0,5,10,15 and 20 dB and bit rate of transmitting data is equal to 1 Mbps for BPSK modulation, so that symbol period T_s is 1 μsec. A forgetting factor of 0.95 for RLS algorithms is adopted based on an optimal result from preliminary performed computer simulation. Considered frequency f is 5 GHz so that wavelength λ is 6 cm. A mobile station is moving with different velocity from 0-120 m/s.

Table 4.3: Simulation Conditions

Carrier to Noise Ratio (CNR)	0,5,10,15 dB
Bit Rate	1 Mbps
Modulation	BPSK
Velocity	0-120 m/s (0-432 km/h)
Frequency (wavelength)	5 GHz (6 cm)
Forgetting Factor	0.95
Number of Basestation Antennas	4 antennas
Power Efficiency ξ	0.7[2]

We first provide simulation results for the conventional scheme given in the previous section when setting $T_p = T_d$. In the case of CNR equal to 5dB and 1 user (see Fig.4.7), for the scheme with velocity of 2m/s, BER is smaller than 10^{-4}. When the velocity increases to 60m/s, BER becomes more than 10^{-3}. In Fig. 4.8, for CNR equal to 15 dB and 2 users, BER is smaller than 10^{-5} for the velocity of 2m/s, and greater than 10^{-4} at the velocity of 40m/s. We can see from both results that when the speed is very low such as 2 m/s, the optimum numbers of pilot and data bits are longer compared to the case of high speed. This is caused by Doppler spreading with velocity growth. However, The number of pilot and data bits ($L_p$andL_d) are too small for example, less than 10. The performance becomes degraded due to insufficient number of data during T_p. Moreover, in fast fading condition the number of pilot and data bits should be small as much as possible. Therefore, this conventional scheme is not suitable for fast fading environment.

Then we provide simulation results for the conventional scheme (Method 2) given in the previous section when CNR equal to 5 dB and 1 user. Fig.4.9 shows BER results of conventional

[2]This value is set for proposed scheme in Fig.4.10-4.21.

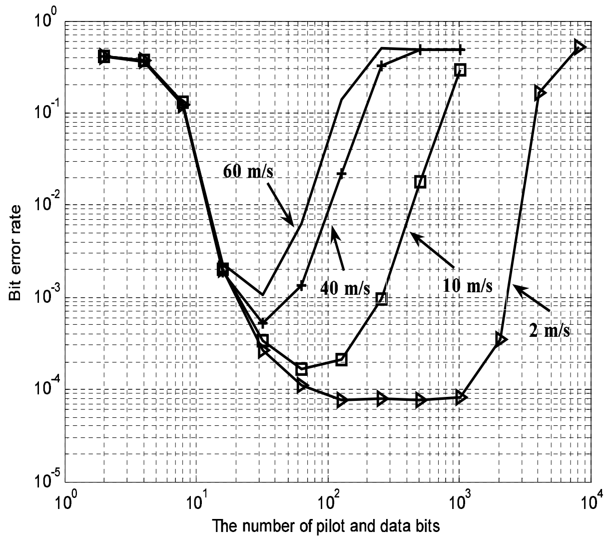

Figure 4.7: BER of conventional MIMO STBC AA method 1 in the case of $T_p = T_d$,1 user ($K = 1$), CNR = 5 dB

transmitting method 2 when setting $L = 1, 2$ and 3 compared to proposed scheme with power efficiency $\xi^{(k)} = 0.5$. It is obviously seen that BER is higher according to the velocity growth and longer data period. This is caused by Doppler spreading with velocity and period expansion. From the figure, proposed method keeps BER of 10^{-3} up to $\beta_0 = 2 \times 10^{-3}$ while conventional method 2 $(L = 1)$ keeps it to $\beta_0 = 10^{-3}$ (i.e, a half value).

Due to simultaneous transmission, power sharing between pilot and information bits need to be examined. Then we evaluate the performance of the proposed method. The power efficiency $\xi^{(k)}$ for 3-users case K is set to 0.7 (=70 percentage) of total power $P_t^{(k)}$, the appropriateness of which is clearly seen from Fig.4.10. Hereafter, we employ ξ of 0.7 for all users cases ($K = 1 - 5$).

After that, we define the optimum forgetting factor of RLS algorithms. As we described this factor in chapter 4, its value is less than or equal one but not less than zero. Even this factor is closer to one, even more the distant past are forgotten. Therefore, we conduct the simulation with various forgetting factor numbers(0.70,0.90,0.92,0.95,0.98) to find the optimum value for this system. Figure 4.11, 4.12, 4.13 and 4.14 show BER performance as a function of CNR at velocity of 20, 30, 50 and 120 m/s respectively. It is obviously seen that at low velocity faogetting factor behave on the theory. With factor equals to 0.98 gives the best BER performance and not much more than that of STBC. However, BER performance of high value forgetting factor (0.95,0.98) increases with velocity expansion but 0.95 does not give high BER. This is due to higher Doppler spread effect in system. From these results, forgetting factor of 0.95 is applied for all speed cases.

From the above results, we can express the performance comparison between conventional scheme (Method2) $L = 1$ and proposed scheme with power efficiency $\xi^{(k)} = 0.7$. In the

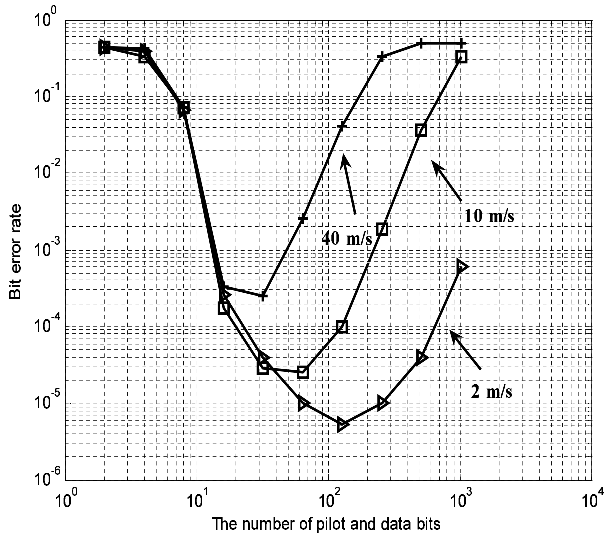

Figure 4.8: BER of conventional MIMO STBC AA method 1 in the case of $T_p = T_d$, 2 users ($K = 2$), CNR = 15 dB

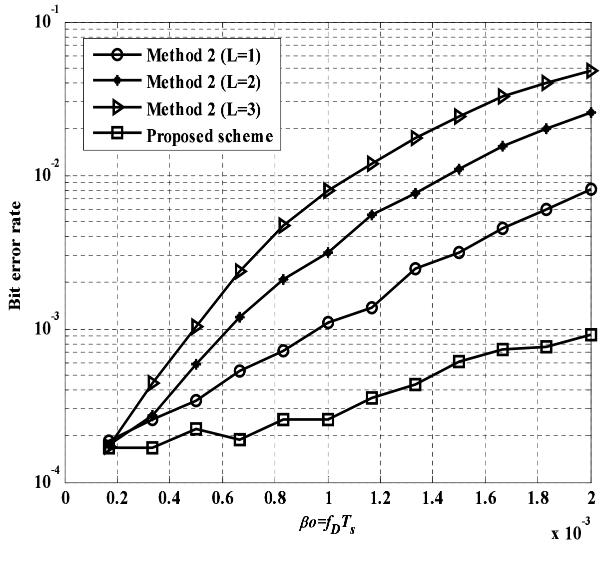

Figure 4.9: BER of the proposed scheme compared with a conventional scheme (Method 2) $L = 1, 2$ and 3 in the case of 1 user ($K = 1$), CNR = 5 dB

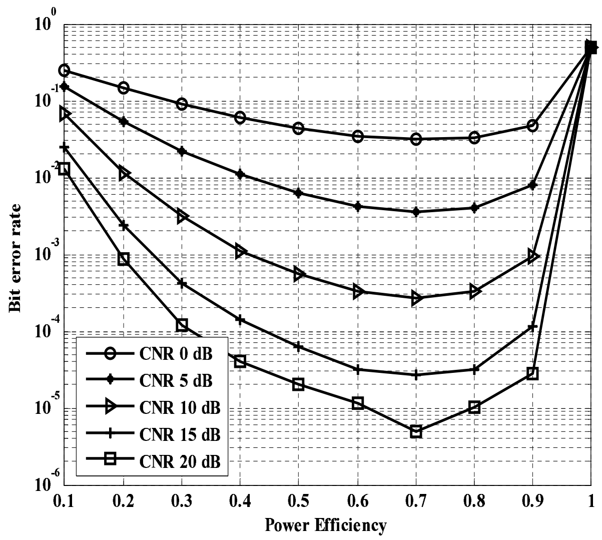

Figure 4.10: BER versus Power Efficiency (ξ) for 3 users (K=3)

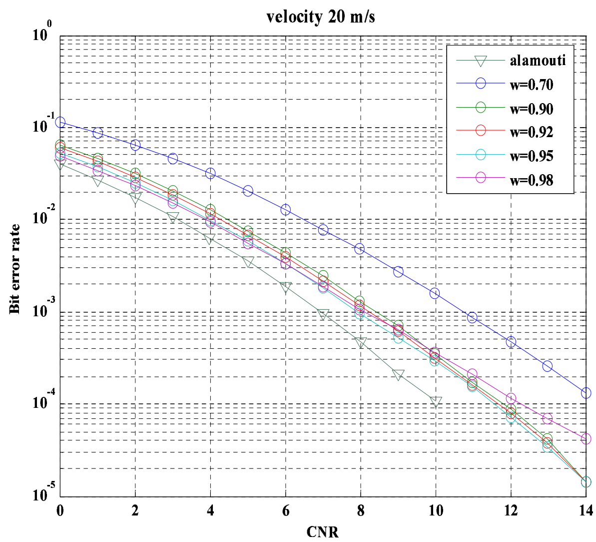

Figure 4.11: BER of various Forgetting Factor of RLS algorithms at velocity of 20 m/s

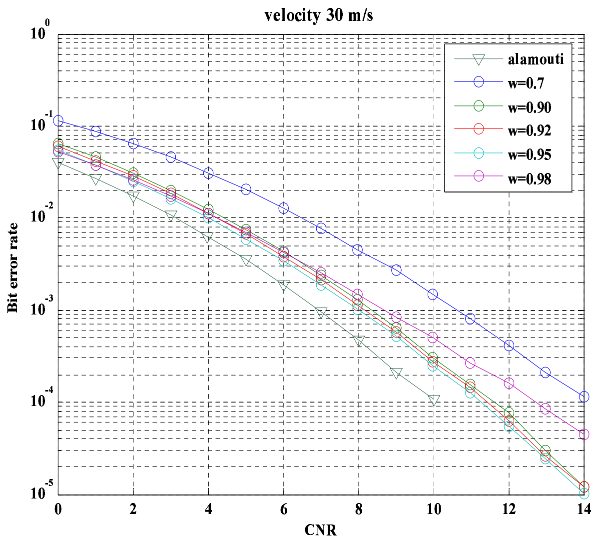

Figure 4.12: BER of various Forgetting Factor of RLS algorithms at velocity of 30 m/s

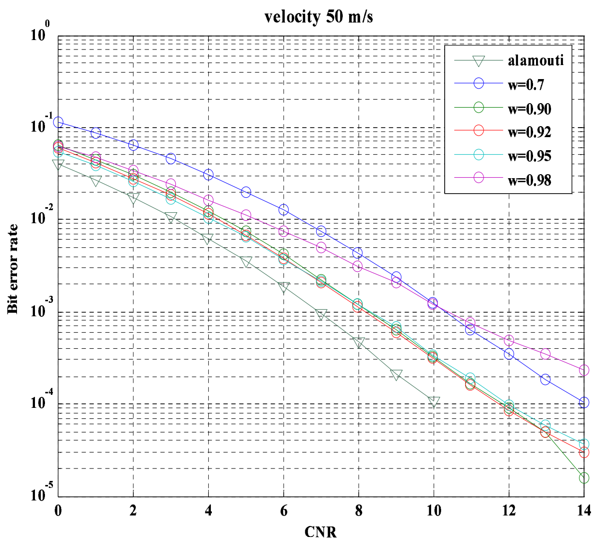

Figure 4.13: BER of various Forgetting Factor of RLS algorithms at velocity of 50 m/s

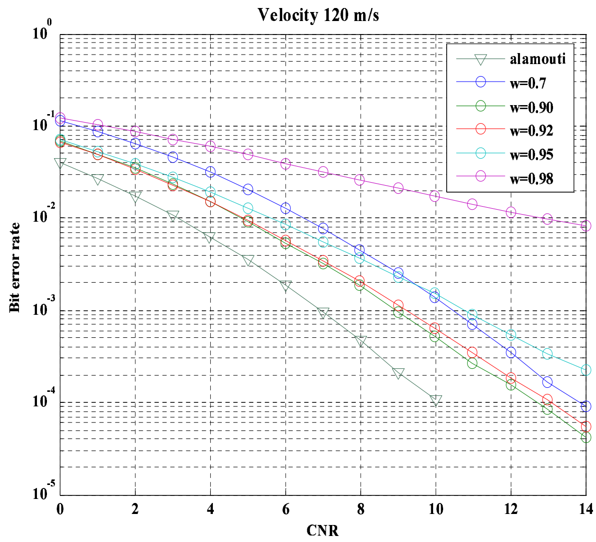

Figure 4.14: BER of various Forgetting Factor of RLS algorithms at velocity of 120 m/s

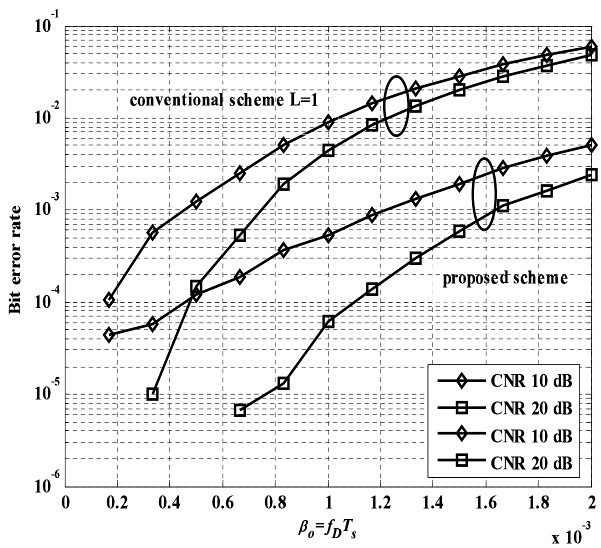

Figure 4.15: BER of the proposed scheme compared with the conventional scheme $(L = 1)$ (method 2) for CNR 10 dB and 20 dB, 3 users $(K = 3)$

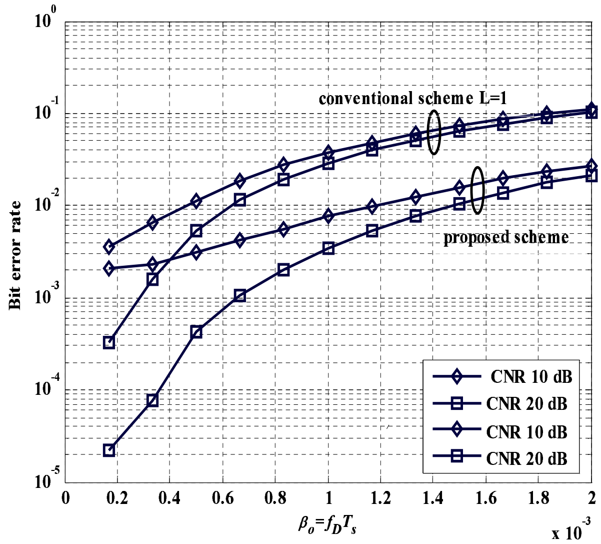

Figure 4.16: BER of the proposed scheme compared with the conventional scheme $(L = 1)$ (method 2) for CNR 10 dB and 20 dB, 4 users $(K = 4)$

case of 3 and 4 users, CNR=10 and 20 dB(see Fig.4.15 and 4.16), proposed scheme at $\beta_0 = 2\times10^{-3}$ gives nearly the same BER performance of conventional schemes for β_0 of around 10^{-3}. According to the results in Fig.4.9, 4.15 and 4.16, the proposed method, the time sequence of which is given in Fig.4.5, has a function to reduce the pilot repetition period effectively. This effect enhances robustness to fast fading, and can extend applicable vehicular speed two times higher than that for conventional method with $L = 1$.

Comparison proposed scheme with conventional method 1 and 2, the results show that conventional method 1 can give good performance in very much lower speed compared to our proposed scheme. Moreover, both length of pilot and data should not be less than 10. This conventional method 1 with using SMI algorithms is not applicable for fast fading environment. In the case of conventional method 2, the performance decreases with increasing number of data bits (L) and speeding up. This method shows the common frame idea which usually sends prior pilot bits. As fast fading channels, it is more severe and difficult to detect signal at the receiver. The result in Fig.4.9 confirms our thoughts and proposed scheme is more applicable for fast fading environments.

Next, we will evaluate BER performance in multi-users system. The propose of this simulation is to investigate how many users and receive antennas can be used in the system. Moreover, how much co-channel interference does effect to each user.

Figure 4.17-4.20 shows BER of 2×4 MIMO STBC AA as a function of fast fading index β_o with parameters of the number of users (K) and CNR. Fig. 4.17 shows the results for one user (K=1). It is seen that CNR $\leq$ 5 dB at velocity = 30 m/s (108 km/h, $\beta_o = 0.0005$) gives bit error rate more than 10^{-5}. When increasing CNR $\geq$ 10 dB, the scheme can absolutely suppress bit error rate.

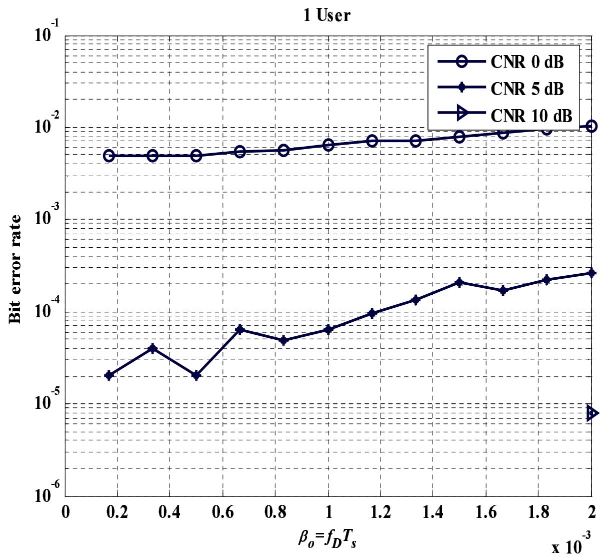

Figure 4.17: BER of the proposed 2×4 MIMO STBC AA scheme in fast fading channel, 1 user ($K = 1$)

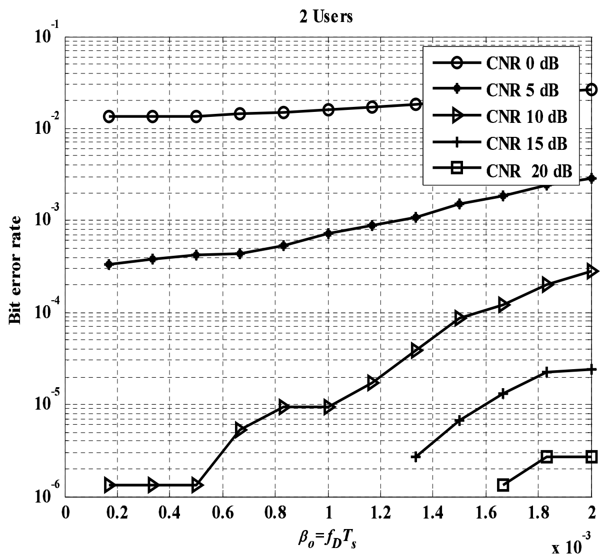

Figure 4.18: BER of the proposed 2×4 MIMO STBC AA scheme in fast fading channel, 2 users ($K = 2$)

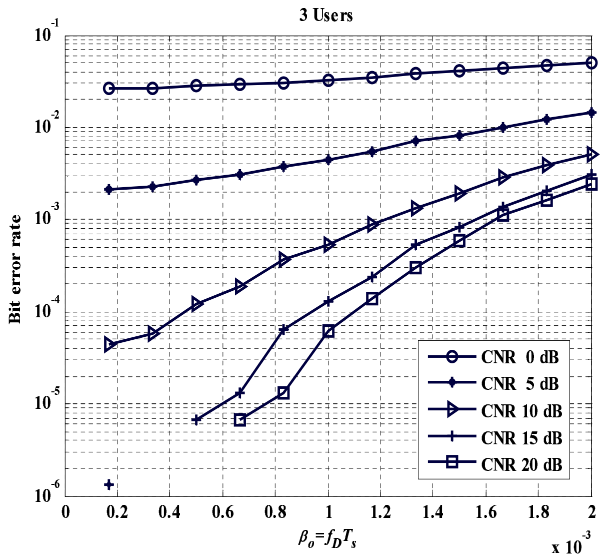

Figure 4.19: BER of the proposed 2×4 MIMO STBC AA scheme in fast fading channel, 3 users ($K = 3$)

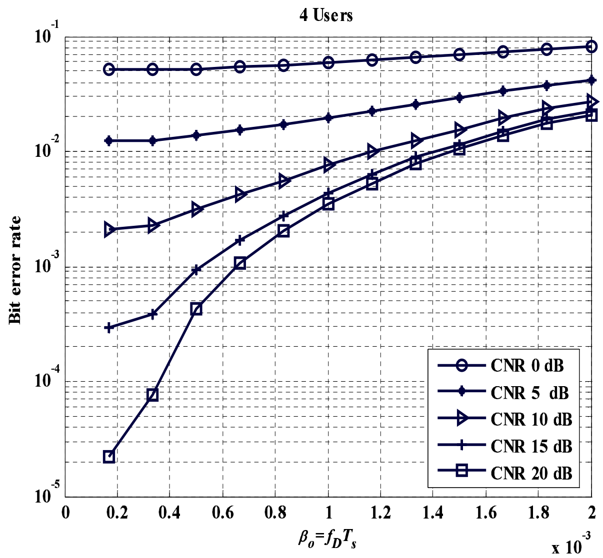

Figure 4.20: BER of the proposed 2×4 MIMO STBC AA scheme in fast fading channel, 4 users ($K = 4$)

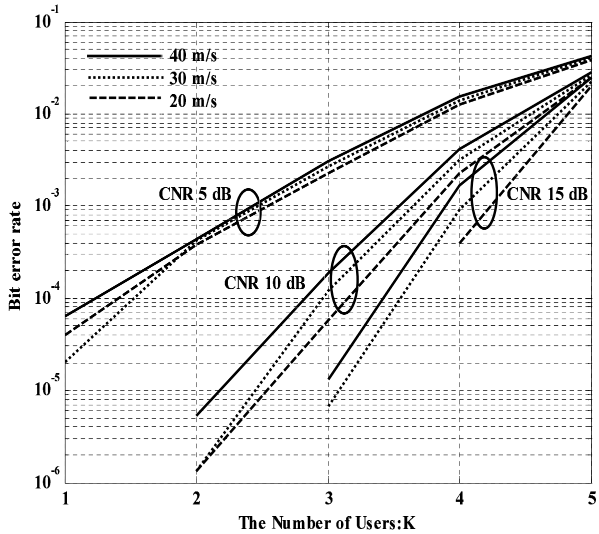

Figure 4.21: BER versus the number of users in different velocity and CNR

In Fig.4.18 for $K = 2$, the result shows that the value of CNR $\leq$ 10 dB at velocity = 50 m/s(180 km/h, $\beta_o = 0.833 \times 10^{-3}$) gives bit error rate $\geq 10^{-5}$ while no errors occur for CNR $\geq$ 15 dB in the system. The results of 3 and 4 users case ($K = 3$ and 4) are illustrated in Fig. 4.19 and 4.20 respectively. In the case of $K = 3$, CNR $\leq$ 15 dB at velocity of 30 m/s gives BER of better than 10^{-5} while $K = 4$ gives BER of more than 10^{-4}.

Figure 4.21 shows the result of BER as a function of the number of users with parameter of velocity (=20,30 and 40 m/s or ($\beta_o = 0.33 \times 10^{-3}, 0.5 \times 10^{-3}$ and 0.0667 respectively)) and CNR(=5,10 and 15 dB). It is obviously realized that in the case of up to 3 users, the system performance improves with increasing CNR but gradually reduces according to velocity increase. It is due to co-channel interference occurred by undesired users leading to reduce system performance. Since the receive array employs $N(=4)$ antenna elements, it can support $N - 1(= 3)$ users. When the number of user exceeds 3, interferences can not be canceled, thus causing the significant performance degradation.

The next simulation is conducted for the diversity gain study. The BER results of 1 and 2 receive antennas with 2 transmit antennas are shown in Fig. 4.22. In the case of 1 receiver, BER can be improved up to 10^{-1} by increasing CNR 5 dB. In the other case(2 receivers), gaining the same value of CNR (5dB) can decrease twice of BER. This result follows diversity gain theory therefore we can assure that our simulations are correct.

Although our proposed method does not utilize CSI directly, more accurate CSI can be incorporated in weight determination with increasing CNR and with decreasing vehicular speed. Therefore, proposed scheme is excellent and outstanding for channel estimation in fast fading environment. As mentioned that proposed scheme has a half rate of the input data rate and this is a weak point. However, we can improve it by adopting higher-rate modulation scheme during data transmission period by utilizing the higher power transmission efficiency in terms of ξ.

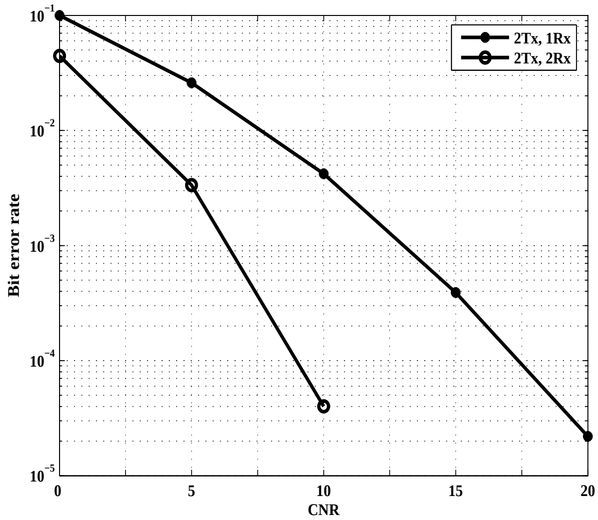

Figure 4.22: BER of one and two receivers with 2 transmitters at very low speed

4.5 Conclusion

In this chapter we have proposed and evaluated an adaptive beamforming scheme for MIMO space-time block coding over fast fading channels. The scheme, which incessantly sends STBC blocks composed of pilot and data signals, can suppress the signal degradation due to Doppler spread effect significantly at high frequency and high velocity conditions. Since the receive array employs N antenna elements, it can effectively accommodate $N - 1$ users without floor errors dut to co-channel interference. In order to identify the basic performance of proposed scheme, we carried out the computer simulation for BPSK transmission system. Accordingly, the research must be extended to improve system performance by optimizing modulation techniques for the future work. Throughout this chapter, we assumed that the synchronization of STBC transmission timing for all mobile terminals is controlled perfectly and that no delay spread is occurred in the channel. Therefore, performance degradation due to imperfectness of the synchronization and its countermeasure schemes are also left as a further study.

Chapter 5

Asynchronous Multi-User MIMO STBC Transmission Scheme in Fast Fading Environment

5.1 Introduction

For synchronous transmission multiuser MIMO STBC systems, we proposed an adaptive beamforming scheme robust to fast fading in Chapter 4 and in[69]. The scheme adopts the simultaneous transmission of data signal and pilot signal which reduces control errors caused by delay of obtaining channel state information (CSI). Data and pilot signals are encoded using space-time block code, while the implementation of adaptive array is considered at the base station to overcome fast fading problem.

All users in [69] are assumed to be synchronous transmission and separated in each group. However, It is high possibility that one user (see Fig.5.1) from another group asynchronously transmit data with focused group and give the interference signals to that group. In order to remove this interference signal, solution must operate based on STBC process for synchronous transmission in focused group. In the case of synchronous transmission multiuser MIMO-STBC systems, signals from K users can be separated in the base station by using K-element array in principle. In the case of asynchronous transmission multiuser MIMO-STBC systems, on the other hand, the number of array elements must be increased depending on relations among block transmission timing of the desired user and those of undesired users. This means that additional co-channel interference (CCI) and inter-symbol interference (ISI) must be taken into account for asynchronous system transmission multi-user MIMO STBC.

In this chapter, we aim to give the application of the spatio-temporal equalization [42] in solving the effects of both ISI and CCI for the Alamouti's STBC transmission systems. The problem of ISI and CCI is canceled simultaneously by proposed tapped delay line adaptive arrays (TDLAA). As mentioned above, our scheme is investigated in fast fading. In order to suppress Doppler spread effect, the sequence of pilot and information data must be different from one in frequency selective fading [42]. For this purpose, using intermittent pilot signals combining weights for data signal are determined with block-by-block signal processing based

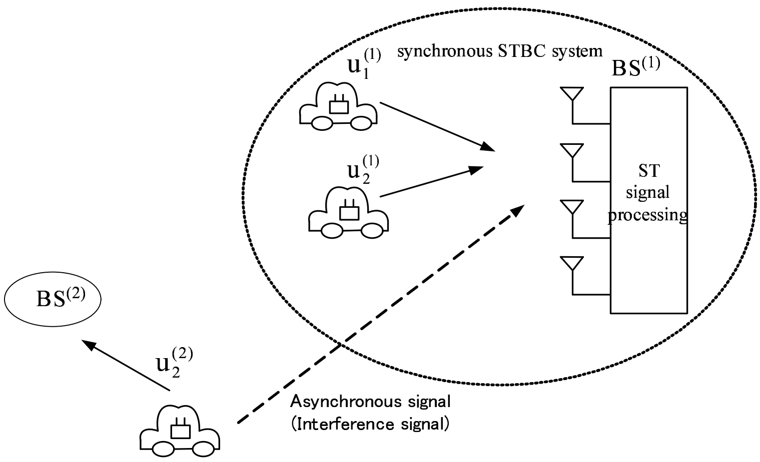

Figure 5.1: The overall image synchronous and asynchronous transmission systems.

on RLS algorithms.

5.2 Definition of Asynchronous Transmission

Inter-Symbol Interference due to Asynchronous Transmission

Asynchronous transmission is explained in Fig.5.2. At the reception timing in the base station with $\Delta T = 0$ between STBC block for user 1 and that for user k, the system is "synchronous". When $0 < \Delta T < T_b (= 2T_s)$, the system becomes "asynchronous". In order to find the worst value of ΔT, we carried out a simulation on BER as a function of ΔT. In this simulation, raised-cosine filtered signal with roll-off factor of 0.5 is used and channels know at the receivers. Fig.5.3 shows the results of BER in the case of 2 users, 2 receive antennas and CNR=15 dB under a quasi-stationary fading condition. From Fig.5.3, it is obviously seen that $0 \leq \Delta T \leq T_s$ BER increases with increasing ΔT but later falling slowly and reaching zero when $\Delta T = 2T_s$. Therefore, at $\Delta T = T_s$or$(\frac{T_b}{2})$ is the worst case for asynchronous transmission. Hereafter we examine only the worst case.

5.3 Configuration and Signal Model

Conventional and Proposed Transmission Method

In this chapter, we consider a case where there are two transmit antennas in each user and P receive antennas at the base station. The encoded transmit signals for both synchronous and asynchronous users are shown in Table 5.1. Moreover Fig.5.4 shows transmitted signal sequence. Frame e contains two pilot symbols with a period of T_b where $T_b = 2T_s$ for weight determination and a number of data ($L = 1, 2$ and 5)with a period of LT_b. At the base station, adaptive arrays with tapped delay line (TDL) is exploited.

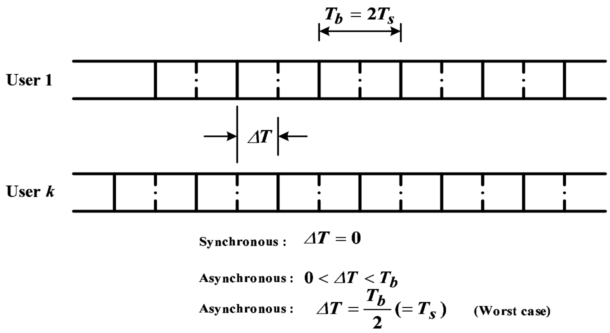

Figure 5.2: The relation of synchronous and asynchronous transmission

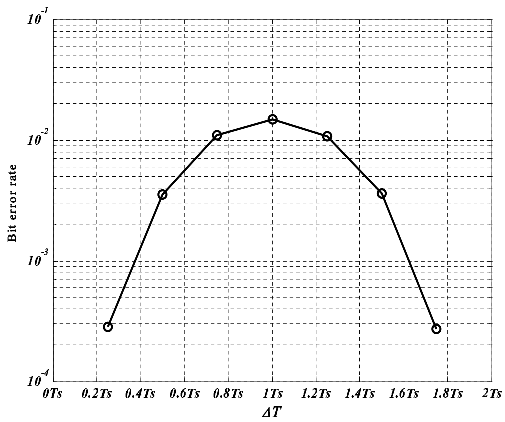

Figure 5.3: BER of various asynchronous conditions in the case of 2 users ($K = 2$), 2 receivers ($P = 2$) and CNR=15dB as a function of ΔT

In order to keep total power of transmission signal be $P_s^{(k)}$, we set

$$< |s_i^{(k)}|^2 >=< |s_{i+1}^{(k)}|^2 >= \frac{1}{2} P_s^{(k)} \tag{5.1}$$

where $< . >$ denotes ensemble average. Table 5.1 is provided for encoded data block $\frac{(i-1)}{2}$, where $i = [1, 3, 5, ...]$. In the case of desired user, signals $s_i^{(k)}$ and $s_{i+1}^{(k)}$ are sent from antenna 1 and 2 respectively for time t, while undesired user signals $-(s_{i+1}^{(k)})^*$ and $(s_i^{(k)})^*$ are sent. For the next symbol time, time $(t + T_s)$, antenna 1 transmits $-(s_{i+1}^{(k)})^*$ and antenna 2 transmits $(s_i^{(k)})^*$ for synchronous user and also in asynchronous user, antenna 1 transmits $s_{i+2}^{(k)}$ and antenna 2 transmits $s_{i+3}^{(k)}$ where $(.)^*$ indicates the complex conjugate. The configuration of the reception side is shown in Fig.5.5. A similar configuration was given in [42] where selective fading environment is assumed in a synchronous system under nearly time-flat fading. With Additive White Gaussian Noise (AWGN) and other user signals, the received signal vector $\boldsymbol{x}$ is given by

Table 5.1: The encoding and transmission sequence for synchronous and asynchronous of user k by comparing the timing of user 1 (=desired user)

time	synchronous		asynchronous	
	antenna1	antenna2	antenna1	antenna2
t	$s_i^{(k)}$	$s_{i+1}^{(k)}$	$-(s_{i+1}^{(k)})^*$	$(s_i^{(k)})^*$
$t+T_s$	$-(s_{i+1}^{(k)})^*$	$(s_i^{(k)})^*$	$s_{i+2}^{(k)}$	$s_{i+3}^{(k)}$

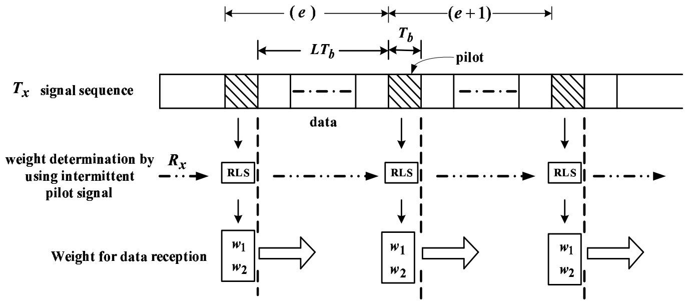

Figure 5.4: Tx signal sequence and weight determination process

$$
\begin{aligned}
\boldsymbol{x}(i) &= \sum_{k=1}^{K}[\boldsymbol{H}^{(k)}(i)\boldsymbol{s}_1^{(k)}(i)] + \boldsymbol{n}(i) \\
&\equiv [x_{11}(i) \quad \ldots \quad x_{P1}(i)]^T
\end{aligned}
\tag{5.2}
$$

$$
\boldsymbol{x}(i+1) = \quad \textstyle\sum_{k=1}^{K}[\boldsymbol{H}^{(k)}(i+1)\boldsymbol{s}_2^{(k)}(i)] + \boldsymbol{n}(i+1) \tag{5.3}
$$

where $(.)^T$ indicates vector transpose and K is total number of users in the system, $\boldsymbol{H}^{(k)}$ is $[P \times 2]$ channel matrix for user k, $\boldsymbol{s}_1^{(k)}$ and $\boldsymbol{s}_2^{(k)}$ are $[2\times1]$ encoding signal vector for user k at time t and $t+T_s$ respectively and $\boldsymbol{n}$ represents $[P\times1]$ noise signal vector.

We can rewrite signals in Eqs. (5.2) and (5.3) in the p receive antenna, where Q is total number of taps in each tapped delay line, as follows

$$
\boldsymbol{y}_p(i) = \left[\; x_{p1}(i) \quad x_{p1}^*(i+1) \quad \ldots \quad x_{p1}(i-(Q-1)) \quad x_{p1}^*(i-(Q-2))]^T \;\right]^T \tag{5.4}
$$

Finally, the reception signal vector can be shown as

$$
\boldsymbol{y}(i) = \left[\; (\boldsymbol{y}_1(i))^T \quad (\boldsymbol{y}_2(i))^T \quad \ldots \quad (\boldsymbol{y}_P(i))^T \;\right]^T \tag{5.5}
$$

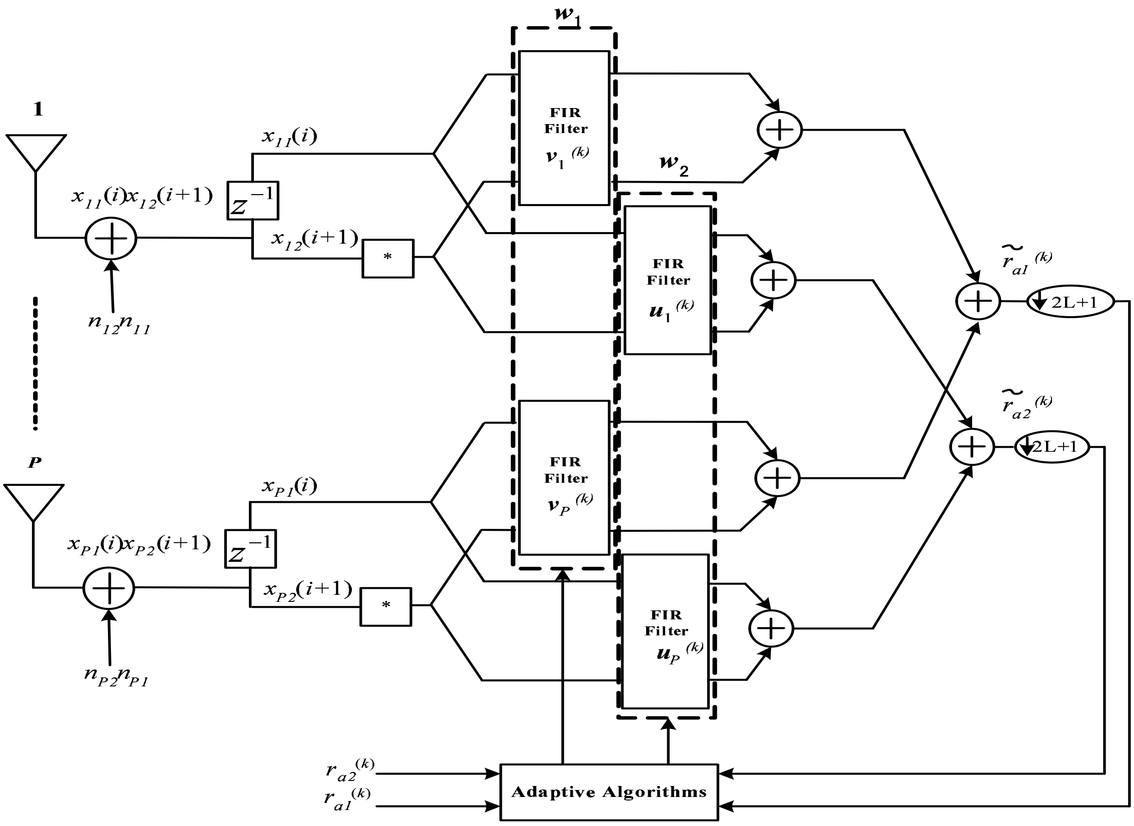

Figure 5.5: MIMO STBC for asynchronous multi-user Adaptive Array for weight determination

The weight vector $\boldsymbol{w}_1^{(k)}$ and $\boldsymbol{w}_2^{(k)}$ in Fig.5.5 for tapped delay line can be expressed in the following equations (see also Fig.5.6) assuming that the 1st $(k = 1)$ user is the desired user.

$$\boldsymbol{w}_1^{(1)} = \left[\begin{array}{cccc} (\boldsymbol{v}_1^{(1)})^T & (\boldsymbol{v}_2^{(1)})^T & \dots & (\boldsymbol{v}_P^{(1)})^T \end{array} \right]^T \tag{5.6}$$

$$\boldsymbol{w}_2^{(1)} = \left[\begin{array}{cccc} (\boldsymbol{u}_1^{(1)})^T & (\boldsymbol{u}_2^{(1)})^T & \dots & (\boldsymbol{u}_P^{(1)})^T \end{array} \right]^T \tag{5.7}$$

where

$$\boldsymbol{v}_p^{(1)} = \left[\begin{array}{ccccc} v_{p1,1}^{(1)} & v_{p2,1}^{(1)} & \dots & v_{p1,Q}^{(1)} & v_{p2,Q}^{(1)} \end{array} \right]^T \tag{5.8}$$

$$\boldsymbol{u}_p^{(1)} = \left[\begin{array}{ccccc} u_{p1,1}^{(1)} & u_{p2,1}^{(1)} & \dots & u_{p1,Q}^{(1)} & u_{p2,Q}^{(1)} \end{array} \right]^T \tag{5.9}$$

The received signals for user 1, $\tilde{s}_i^{(1)}$ and $\tilde{s}_{i+1}^{(1)}$, are given by

$$\tilde{s}_i^{(1)} = (\boldsymbol{w}_1^{(1)})^H \boldsymbol{y}(i) \tag{5.10}$$

$$\tilde{s}_{i+1}^{(1)} = (\boldsymbol{w}_2^{(1)})^H \boldsymbol{y}(i) \tag{5.11}$$

The weight vectors, $w_1^{(1)}$ and $\boldsymbol{w}_2^{(1)}$ are renewed every $(L+1)T_b$ period by using intermittently-inserted pilot block signals (see Fig.5.4). Since received signal vector $\boldsymbol{y}(a)$ where $a = (e-1)(L+1)+1$ includes pilot signal blocks intermittently, the weight is calculated only during the period. Therefore, the reception signal vector $\boldsymbol{y}(a)$ and $[2QP \times 1]$ weight vector $\boldsymbol{w}_1^{(1)}$ are then combined to produce estimated pilot outputs $\tilde{r}_{a1}^{(1)}$ and $\tilde{r}_{a2}^{(1)}$. They are given by

$$\tilde{r}_{a1}^{(1)} = (\boldsymbol{w}_1^{(1)})^H(a)\boldsymbol{y}(a) \tag{5.12}$$

$$\tilde{r}_{a2}^{(1)} = (\boldsymbol{w}_2^{(1)})^H(a)\boldsymbol{y}(a) \tag{5.13}$$

where $(.)^H$ is the complex conjugate transpose. This is considered to be type of $r_{a1}^{(1)}, r_{a2}^{(1)}$ because $\tilde{r}_{a1}^{(1)}$ and $\tilde{r}_{a2}^{(1)}$ are already defined as estimated pilot outputs.

$$\boldsymbol{w}_{1_{opt}}^{(1)}(a) = \arg\min < |r_{a1}^{(1)} - (\boldsymbol{w}_1^{(1)})^H(a)\boldsymbol{y}(a)|^2 > \tag{5.14}$$

The optimal weight $\boldsymbol{w}_{1_{opt}}^{(k)}(i)$ is time-variant and referred to optimum Wiener solution.

$$\boldsymbol{w}_1^{(1)}(a) = \boldsymbol{R}_1^{-1}(a)\boldsymbol{b}_1^{(1)}(a) \tag{5.15}$$

$$\boldsymbol{R}_1(a) = \gamma\boldsymbol{R}_1(a-1) + \boldsymbol{y}(a)\boldsymbol{y}^H(a) \tag{5.16}$$

$$\boldsymbol{b}_1^{(1)}(a) = \gamma\boldsymbol{b}_1^{(1)}(a-1) + (r_{a1}^{(1)})^*\boldsymbol{y}(a) \tag{5.17}$$

where $\boldsymbol{R}_1$ is usually referred to as the correlation matrix. In this chapter, we adopt Recursive Least Squares (RLS) algorithm to obtain weight vector $\boldsymbol{w}_1^{(1)}$. The forgetting factor $0 < \gamma < 1$ is a parameter of the RLS algorithm, and intends to follow temporal variation of Channel State Information (CSI). The weight vector $\boldsymbol{w}_2^{(1)}$ can also be obtained for estimating $\tilde{r}_{i2}^{(1)}$ by doing similarly as in Equations (5.15)-(5.17), and is given by

$$\boldsymbol{w}_{2_{opt}}^{(1)}(a) = \arg\min < |r_{a2}^{(1)} - (\boldsymbol{w}_2^{(1)})^H(a)\boldsymbol{y}(a)|^2 > \tag{5.18}$$

The time varying channel characteristic $\boldsymbol{H}^{(k)}(i)$ for data block(i), user k can be written in matrix form as

$$\boldsymbol{H}^{(k)}(i) = \begin{bmatrix} h_{1,1}^{(k)}(i) & h_{1,2}^{(k)}(i) \\ \vdots & \vdots \\ h_{P,1}^{(k)}(i) & h_{P,2}^{(k)}(i) \end{bmatrix} \tag{5.19}$$

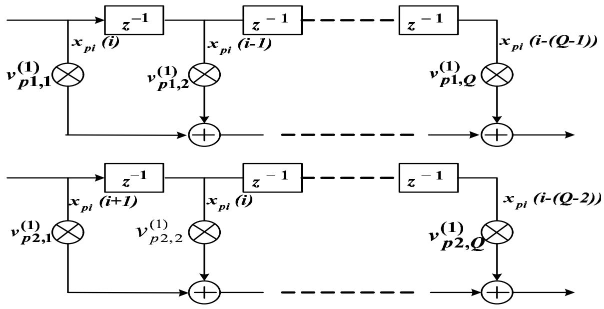

Figure 5.6: A finite impulse response (FIR) without controlling weights

The average channel power gain is set to 1 as follows

$$< |h_{11}^{(k)}|^2 >=< |h_{12}^{(k)}|^2 >= \ldots =< |h_{P2}^{(k)}|^2 >= 1 \tag{5.20}$$

Data signal power $P_s^{(k)}$ and pilot signal power $P_r^{(k)}$ are equally allocated in this chapter. Noise signals shown in Eqs. (5.2) and (5.3) can be explained in average power gain as follows

$$P_n =< |n_{11}|^2 >=< |n_{12}|^2 >= \ldots =< |n_{P2}|^2 > \tag{5.21}$$

The ratio of noise power P_n and total power $P_t^{(k)}$ intends to show input $CNR^{(k)}$ calculation for the system as follows:

$$CNR^{(k)} = \frac{P_t^{(k)}}{P_n} \tag{5.22}$$

5.4 Simulation and Results

In our simulation, we generate i.i.d. Rayleigh fading channel having Jakes-type power spectrum [45] based on Eq.(5.2). Simulation conditions are summarized in Table 5.2.

$CNR^{(k)}$ is set to be equal to all users k in this chapter therefore it can be easily rewritten in CNR.By adopting RLS algorithm with forgetting factor γ of 0.95, the effective number of iterations, m, is estimated to be 15. Figure 5.7-5.12 shows BER of 2 users ($K = 2$) as a function of CNR in different 3 cases, namely, Case 1 is synchronous transmission between the two users, Case 2 is asynchronous transmission and reception without TDLs, and Case 3 is the same as case 2 but with TDLs(Q=2). It is obviously seen that the BER performance accordingly improves with increasing CNR fairly up to CNR=20 dB while it becomes saturation probably due to effect of irreducible CCI. The asynchronous transmission (Case2) gives larger BER than synchronous transmission (Case1). However, it can be solved by adding tapped delay line at the receiver side.

According to the result (CNR=30dB and $\beta_0 = 5 \times 10^{-4}$) the tapped delay line system (Case 3) can reduce BER from 2×10^{-2} to 4×10^{-3} and BER is rather similar to synchronous system

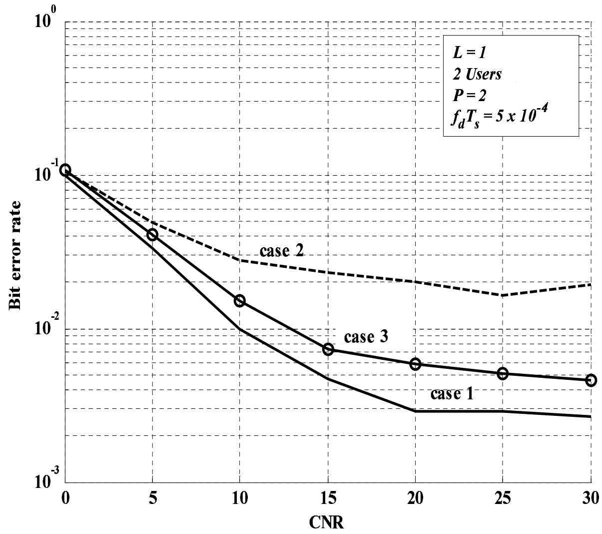

Figure 5.7: BER of the proposed asynchronous MIMO STBC AA scheme in fast fading channel $K = 2$ (2users), 2 receivers ($P = 2$) with $\beta_0 = 5 \times 10^{-4}(v = 30m/s)$

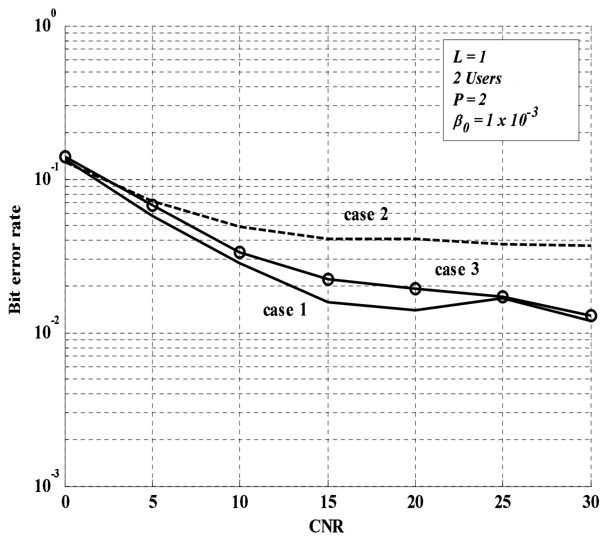

Figure 5.8: BER of the proposed asynchronous MIMO STBC AA scheme in fast fading channel $K = 2$ (2users), 2 receivers ($P = 2$) with $\beta_0 = 1 \times 10^{-3}(v = 60m/s)$

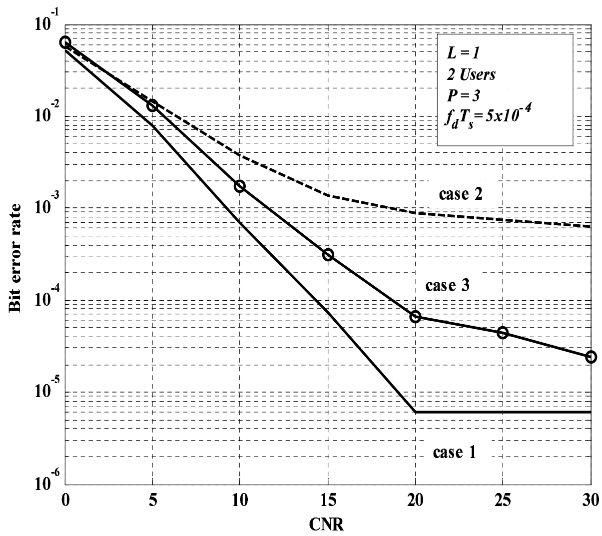

Figure 5.9: BER of the proposed asynchronous MIMO STBC AA scheme in fast fading channel $K = 2$ (2users),3 receivers ($P = 3$) with $\beta_0 = 5 \times 10^{-4} (v = 30m/s)$

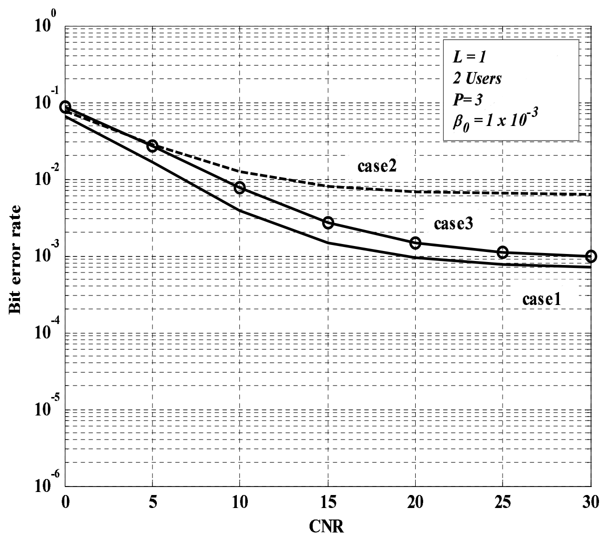

Figure 5.10: BER of the proposed asynchronous MIMO STBC AA scheme in fast fading channel $K = 2$ (2users),3 receivers ($P = 3$) with $\beta_0 = 1 \times 10^{-3} (v = 60m/s)$

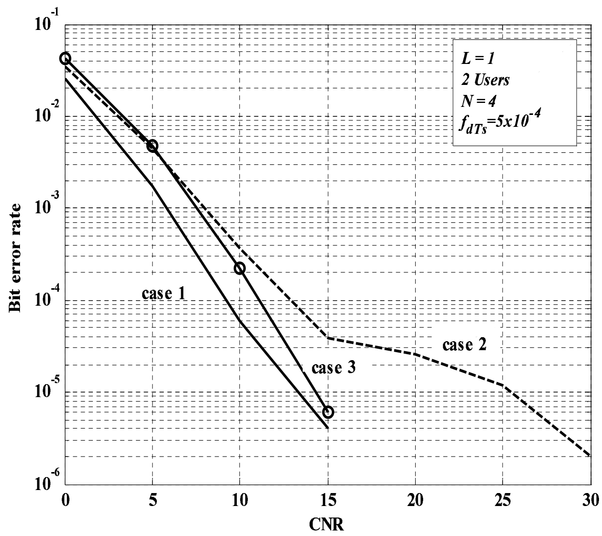

Figure 5.11: BER of the proposed asynchronous MIMO STBC AA scheme in fast fading channel $K = 2$ (2users),4 receivers ($P = 4$) with $\beta_0 = 5 \times 10^{-4} (v = 30m/s)$

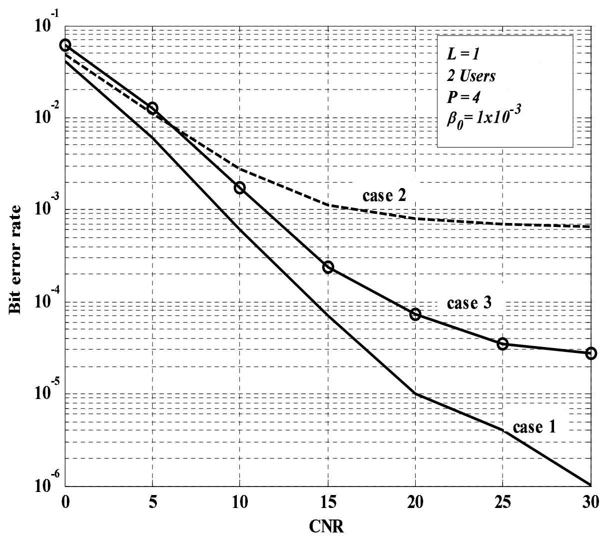

Figure 5.12: BER of the proposed asynchronous MIMO STBC AA scheme in fast fading channel $K = 2$ (2users), 4 receivers ($P = 4$) with $\beta_0 = 1 \times 10^{-3} (v = 60m/s)$

Table 5.2: Simulation Conditions

Carrier to Noise Ratio (CNR)	0-30dB
Modulation	BPSK
β_0:$f_D T_s$	10^{-4}-10^{-2}
Forgetting Factor	0.95
Number of Total Users K	2, 3
Data block length L	1,2,5
Number of Taps Q	1,2,3
Number of BS antennas P	2-4

for $P = 2$ (Fig.5.7). While for $P = 3$ (Fig.5.9), BER from 6×10^{-4} to 2×10^{-5} and $P = 4$ (Fig.5.11), it can suppress BER undetectable level. For the result of $\beta_0 = 1 \times 10^{-3}$ with $P = 2$, $P = 3$ and $P = 4$, can reduce BER from 3×10^{-1} to 1×10^{-2} with reference to Fig.5.8, from 6×10^{-3} to 1×10^{-3} with reference to Fig.5.10 and from 6×10^{-3} to 3×10^{-5} with reference to Fig.5.12. As seen from these results, higher velocity conditions give more bit error rate than lower speed conditions. This caused by high doppler spread at high speed.

Figure 5.13 shows results of transmitting method when setting data block length $L = 1, 2, 5$ (see Fig.5.4) as a function of β_0 It is clearly seen that at BER around 5×10^{-5} scheme with $L = 1$ can extend applicable vehicular speed two and ten times higher than that for $L = 2$ and 5. According to this result, the proposed method with $L = 1$ enhances robustness to fast fading although data rate becomes half. Accordingly we adopted $L = 1$ with $\beta_0 = 5 \times 10^{-4} (v = 30\text{m/s})$ for Fig.5.7),5.9,5.11 and (e) and with $\beta_0 = 10^{-3} (v = 60\text{m/s})$ for Fig.5.8,5.10 and 5.12

Figure 5.14-5.16 shows BER performance versus CNR when varying Q from 1 to 3 in different velocity ($v = 30, 60$ and 90 m/s $\beta_0 = 5 \times 10^{-4}$, $\beta_0 = 10^{-3}$ and $\beta_0 = 1.5 \times 10^{-3}$). Q is the number of delay taps (see Fig.5.5). We can see from the results that the case of $Q = 3$ gives nearly the same BER performance as that of $Q = 2$ and the velocity changing does not effect to these relations. Accordingly the proposed scheme with number of tapped delay with $Q = 2$ is effective for the system.

Next we evaluated BER performance of the scheme for three-user case ($K = 3$). In Fig.5.17, Case 2 is two asynchronous users ($K_a = 2$) and is received without TDLs(Q=1), while Case 3 is those with TDLs(Q=2). Case 1 is three synchronous users for the reference of comparison. Also in Fig.5.18, Case 2 is one asynchronous user ($K_a = 1$) and is received without TDLs(Q=1), while Case 3 is those with TDLs(Q=2). Case 1 is the same as that in Fig.5.17.In both figures, the number of receiving antenna is 4 ($P = 4$), and other parameter values are given in the figures.

In the case of two asynchronous users, since each user transmits two CCI signals, receiving station has to cancel four CCI signals in total. Therefore Case 2 of Fig.5.17 with $P = 4$ is apparently beyond the degree of freedom of the array for cancellation. For Case 3, with the help of equalization by TDL this limitation is reduced. However, considerable degradation for Case 3 can be observed compared with Case 1. On the other hand, in the case of one asynchronous user, TDL can reduce CCI in Case 2 and give BER nearly the same as in Case 1 (see Fig.5.18). This means two CCI signals can be decreased by adding one tapped delay line.

In the next simulation, we explore performance of the proposed scheme in a multi-receiving

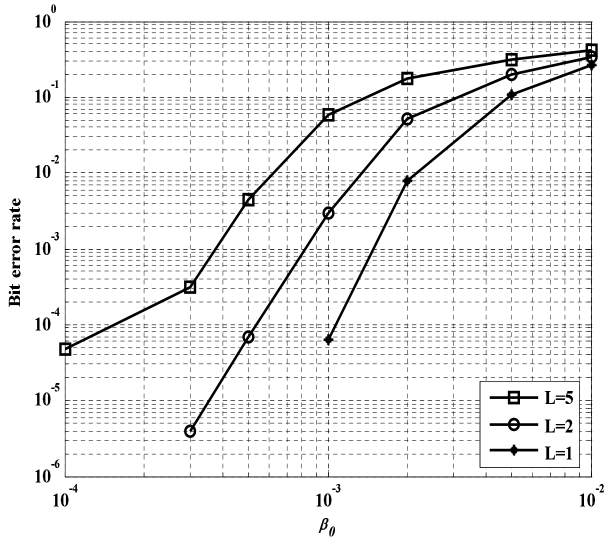

Figure 5.13: BER of the scheme with $L = 1, 2$ and 5 in the case of 3 users($K = 3$), 4 receivers($P = 4$) and CNR=20dB

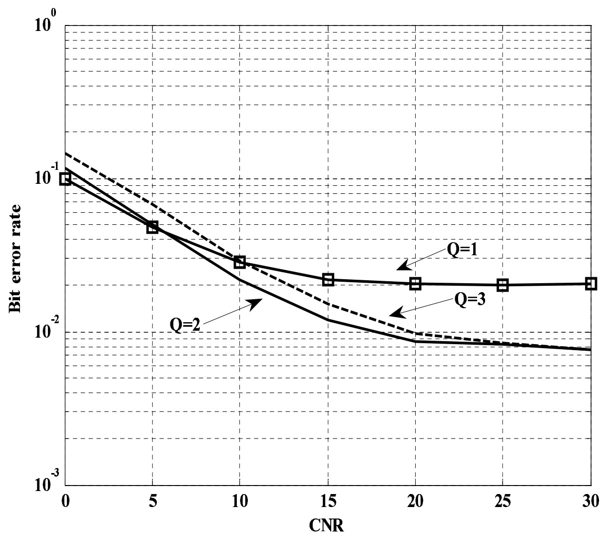

Figure 5.14: BER of the proposed in fast fading with 2 users ($K = 2$) 3 receivers ($P = 3$) $\beta_0 = 5 \times 10^{-4}(v = 30m/s)$

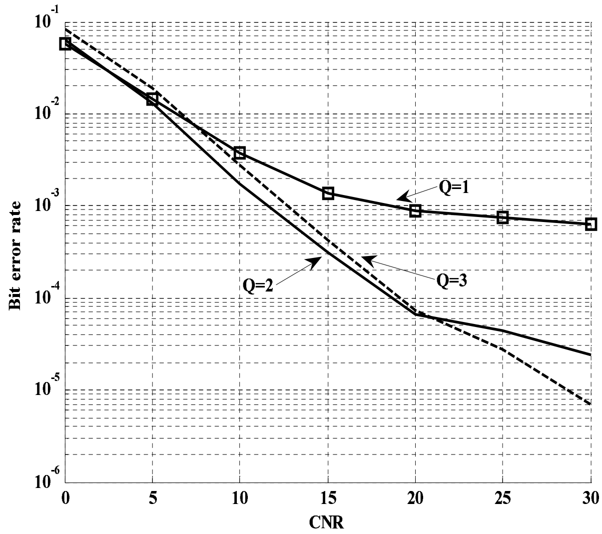

Figure 5.15: BER of the proposed in fast fading with 2 users ($K = 2$) 3 receivers ($P = 3$) $\beta_0 = 1 \times 10^{-3}(v = 60m/s)$

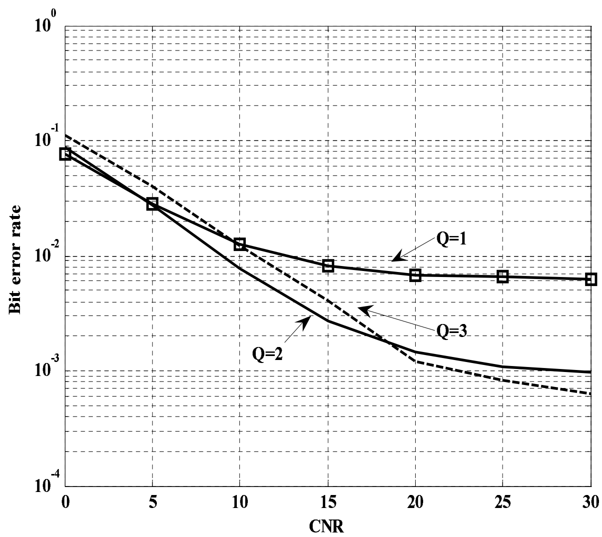

Figure 5.16: BER of the proposed in fast fading with 2 users ($K = 2$) 3 receivers ($P = 3$) $\beta_0 = 1.5 \times 10^{-3}(v = 90m/s)$

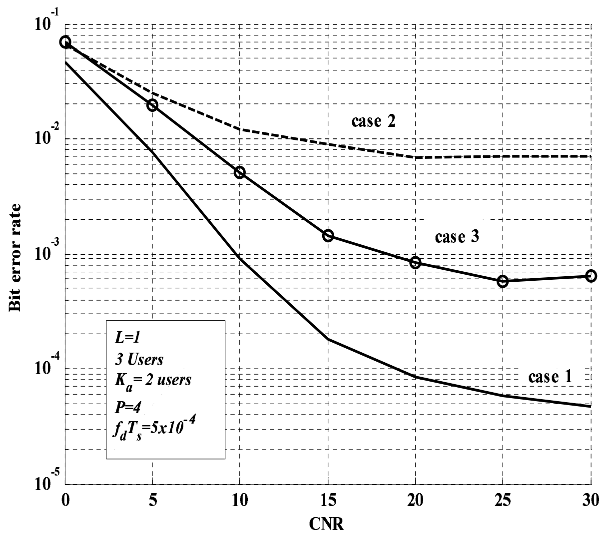

Figure 5.17: BER characteristic for 3 users ($K = 3$) with $\beta_0 = 5 \times 10^{-4}(v = 30m/s)$

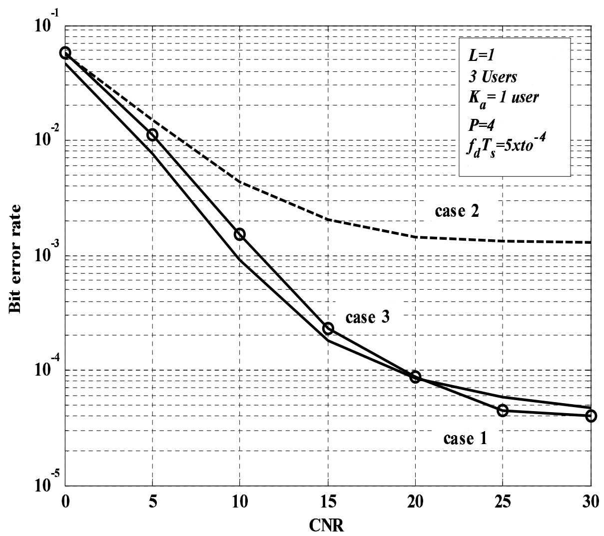

Figure 5.18: BER characteristic for 3 users ($K = 3$) with $\beta_0 = 5 \times 10^{-4}(v = 30m/s)$

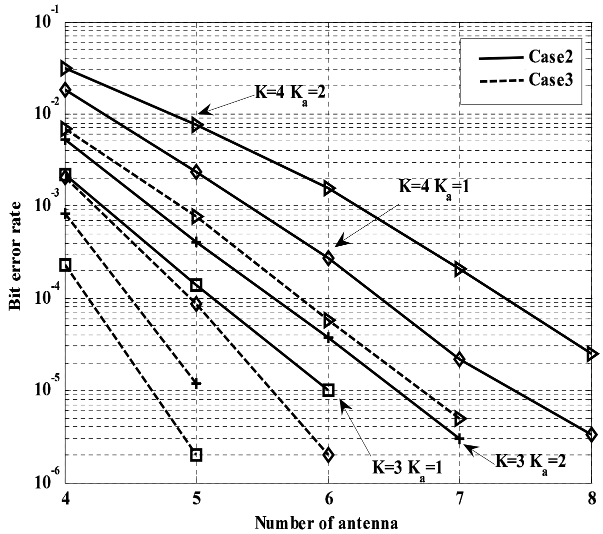

Figure 5.19: BER characteristic for 3 and 4 users in the function of receiving antenna numbers

antenna. The purpose of the simulation is to see how much TDL can suppress co-channel interference, or equivalently how many total users and asynchronous users with and without TDLs can be accommodated. In Fig.5.19, BER of the proposed scheme is illustrated for three and four users ($K = 3$ and 4) with receiving antennas varying from four to eight ($P = 4 - 8$). Case 2 is system with one and two asynchronous users while Case 3 is those with TDLs(Q=2). It is immediately realized from the figure that as the number of users increases, the performance in case 3 is higher. Moreover, in the case of four users, two asynchronous users ($K = 4$, $K_a = 2$) with TDLs(Q=2) give BER performance nearly the same as in the case of three users, two asynchronous users ($K = 3$, $K_a = 2$) without TDLs. On the other case, four users, one asynchronous user ($K = 4$, $K_a = 1$) with TDLs(Q=2) also can suppress CCI as good as in the case of three users, one asynchronous user ($K = 3$, $K_a = 1$) without TDLs.

We can see from the results that BER increases according to the total number of users and asynchronous users in the system but gradually reduce with bigger CNR and number of receivers. This is due to the fact that since undesired and asynchronous users are treated as co-channel interferences. CCI cancellation can be provided by adding TDLs into system. As for estimation of user accommodation capability, a general formula as a function of K, K_a and P must be developed, but it is left as a future study.

5.5 Conclusion

In this chapter we have proposed and evaluated asynchronous transmission MIMO space-time block coding adaptive array with tapped delay line in fast fading channels. The scheme, which uses intermittent pilot signals and combining weight for data signal block-by-block, can effectively suppress the signal degradation due to CCI and Doppler spread effect significantly. In order to identify the basic performance of proposed scheme, we carried out the computer simulation for BPSK transmission system. It was also shown that the preferable number of tapped delay line is 2 for asynchronous transmission. Moreover, by adopting alternate transmission of pilot signal and information signal with $L = 1$ can achieve BER of smaller than 10^{-4} at $f_D T_s = 10^{-3}$ in an asynchronous transmission case. Further study on performance evaluation for both synchronous and asynchronous transmission multi-user systems must be necessary for double-selective multipath conditions, namely, time-selective and frequency-selective fading conditions

Chapter 6

Conclusion and Future Work

This chapter summarizes the results of this work and describes open topics for the future research. Finally, conclusion of the work is included.

6.1 Conclusions

In this work, small scale fading and its model were reviewed in Chapter 2. Chapter 3 described overview of MIMO and discussed space time block coding. Performance of Synchronous multi-user MIMO STBC AA was analyzed using theoretical method in Chapter 4. Finally, MIMO STBC AA for asynchronous transmission over fast fading was presented in Chapter 5.

According to the numerical and simulation results shown in this work, the following concluding remarks are obtained

Performance of Synchronous Multi-user transmission scheme

1. Detailed mathematical models for performance analysis of multi-user synchronous transmission scheme was successfully developed. The models give exact expressions for proposed scheme, power efficiency, performance comparison between proposed scheme and conventional scheme and optimum number users. The developed model is simple and can be applied for transmission system and enhances robustness to fast fading channels

2. It was shown that in the case of up to 3 users, the system performance improves with increasing CNR but gradually reduces according to velocity increase. It is due to co-channel interference occurred by undesired users leading to reduce system performance. Since the receive array employs $N(=4)$ antenna elements, it can support $N-1(=3)$ users. When the number exceeds 3, interferences can not be canceled, thus causing the significant performance degradation.

3. Our method does not utilze CSI directly, but using weight determination by increasing CNR and vehicular speed. Therefore, proposed scheme is excellent and outstanding for channel estimation in fast fading environment.

4. Proposed scheme has a half rate of the input data rate but it can be improved by adopting higher-rate modulation scheme during data transmission period by utilizing the higher power transmission efficiency.

Performance of Asynchronous Multi-user transmission scheme

1. we evaluated asynchronous transmission MIMO space-time block coding adaptive array with tapped delay line in fast fading channels. The scheme, which uses intermittent pilot signals and combining weight for data signal block-by-block, can effectively suppress the signal degradation due to CCI and Doppler spread effect significantly.

2. Since undesired and asynchronous users are treated as co-channel interferences. CCI cancellation can be provided by adding TDLs into system. One asynchronous user has two CCI signals which can be decreased by adding one tapped delay line ($Q = 2$).

3. By adopting alternate transmission of pilot signal and information signal with one of data block length ($L = 1$) can achieve BER of smaller than 10^{-4} at $f_D T_s = 10^{-3}$ in an asynchronous transmission case.

6.2 Future Work

Referring to the above conclusions, there are several areas of this work which could be extended for future research.

1. As for estimation of user accommodation capability, a general formula as a function of K, K_a and P must be developed

2. Performance evaluation for both synchronous and asynchronous transmission multi-user systems must be necessary for double-selective multipath conditions, namely, time-selective and frequency-selective fading conditions

3. In this thesis, scheme with two transmit antennas have been proposed. However, transmitting with more than two antennas is left for an interesting future study.

4. The scheme with modulated by higher rate modulation (QPSK,16QAM) and included with pilot is also an interesting scheme.

Appendix A

Derivation of $\boldsymbol{w}_1$ and $\boldsymbol{w}_2$

In order to derive weight vectors, we assume single user with two receivers as shown in Fig.A.1. After additive white gaussian noise, the signals from transmitted antennas in the 1st and 2nd receive antenna are given by (referenced from Eq.4.6 and 4.7)

$$x_{11}(i) = r_i h_{11} + s_i h_{12} + n_{11} \tag{A.1}$$

$$x_{12}^*(i) = -s_i h_{11}^* + r_i h_{12}^* + n_{12}^* \tag{A.2}$$

$$x_{21}(i) = r_i h_{21} + s_i h_{22} + n_{21} \tag{A.3}$$

$$x_{22}^*(i) = -s_i h_{21}^* + r_i^* h_{22} + n_{22}^* \tag{A.4}$$

Receive signals from Eq.A.1,A.2,A.3 and A.4 are then sent through two weight vectors as shown in Fig.A.1 and the operation can be shown as

$$x_{11}(i) h_{11}^* = r_i h_{11} h_{11}^* + s_i h_{12} h_{11}^* + n_{11} h_{11}^* \tag{A.5}$$

$$x_{12}^*(i) h_{12} = -s_i h_{11}^* h_{12} + r_i h_{12}^* h_{12} + n_{12}^* h_{12} \tag{A.6}$$

$$x_{21}(i) h_{21}^* = r_i h_{21} h_{21}^* + s_i h_{22} h_{21}^* + n_{21} h_{21}^* \tag{A.7}$$

$$x_{22}^*(i) h_{22} = -s_i h_{21}^* h_{22} + r_i h_{22}^* h_{22} + n_{22}^* h_{22} \tag{A.8}$$

We combine Eq.A.5,A.6,A.7 and A.8 to obtain $\tilde{r}_i$ as following equation.

$$\begin{aligned}
\tilde{r}_i &= x_{11}(i) h_{11}^* + x_{12}^*(i) h_{12} + x_{21}(i) h_{21}^* + x_{22}^*(i) h_{22} \\
&= r_i h_{11} h_{11}^* + r_i h_{12}^* h_{12} + r_i h_{21} h_{21}^* + r_i h_{22}^* h_{22} + n_{11} h_{11}^* + n_{12}^* h_{12} + n_{21} h_{21}^* + n_{22}^* h_{22} \\
&= (h_{11}^2 + h_{12}^2 + h_{21}^2 + h_{22}^2) r_i + n_{11} h_{11}^* + n_{12}^* h_{12} + n_{21} h_{21}^* + n_{22}^* h_{22}
\end{aligned} \tag{A.9}$$

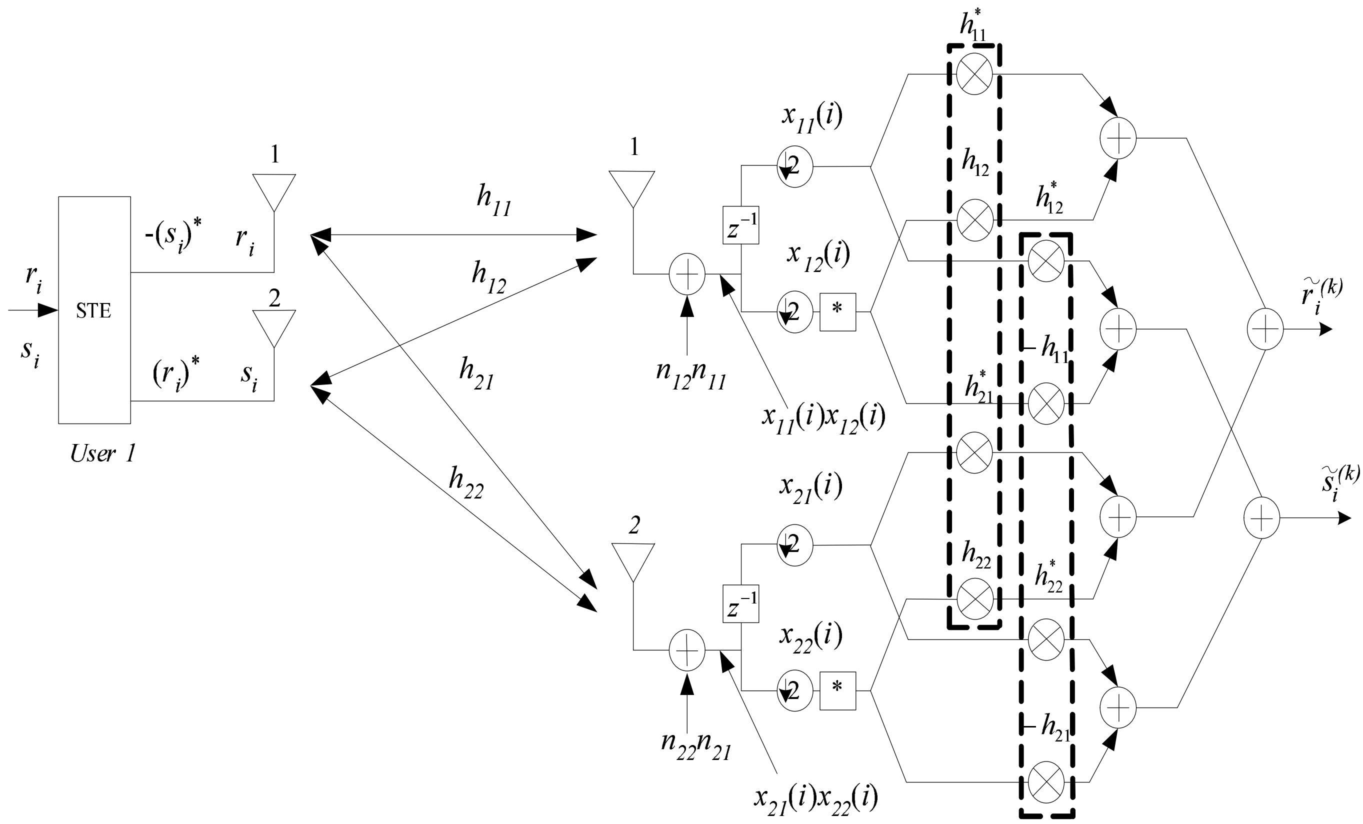

Figure A.1: Adaptive beamforming configuration for single user

In similar idea, obtaining $\tilde{s}_i$ as following equations.

$$x_{11}(i)h^*_{12} = r_i h_{11} h^*_{12} + s_i h_{12} h^*_{12} + n_{11} h^*_{12} \tag{A.10}$$

$$-h_{11} x^*_{12}(i) = h_{11} s_i h^*_{11} - h_{11} r_i h^*_{12} - h_{11} n^*_{12} \tag{A.11}$$

$$x_{21}(i)h^*_{22} = r_i h_{21} h^*_{22} + s_i h_{22} h^*_{22} + n_{21} h^*_{22} \tag{A.12}$$

$$-h_{21} x^*_{22}(i) = h_{21} s_i h^*_{21} - h_{21} r_i h^*_{22} - h_{21} n^*_{22} \tag{A.13}$$

Finally, we get $\tilde{s}_i$ as the output signal.

$$\begin{aligned}
\tilde{s}_i &=_{11} (i)h^*_{12} - h_{11} x^*_{12}(i) + x_{21}(i) h^*_{22} - h_{21} x^*_{22}(i) \\
&= s_i h_{12} h^*_{12} + h_{11} s_i h^*_{11} + s_i h_{22} h^*_{22} + h_{21} s_i h^*_{21} + n_{11} h^*_{12} - h_{11} n^*_{12} + n_{21} h^*_{22} - h_{21} n^*_{22} \\
&= (h^2_{11} + h^2_{12} + h^2_{21} + h^2_{22}) s_i + n_{11} h^*_{12} - h_{11} n^*_{12} + n_{21} h^*_{22} - h_{21} n^*_{22}
\end{aligned} \tag{A.14}$$

Considering weight vectors $\boldsymbol{w}_1$ and $\boldsymbol{w}_2$, we see the relation between both.

$$\boldsymbol{w}_1 = \begin{bmatrix} h_{11}^* & h_{12} & h_{21}^* & h_{22} \end{bmatrix}^T \tag{A.15}$$

$$\boldsymbol{w}_2 = \begin{bmatrix} h_{12}^* & -h_{11} & h_{22}^* & -h_{21} \end{bmatrix}^T \tag{A.16}$$

We can conclude and remark their relations as follow.

$$\boldsymbol{w}_1 = \begin{bmatrix} w_{11} & w_{12} & w_{21} & w_{22} \end{bmatrix}^T \tag{A.17}$$

$$\boldsymbol{w}_2 = \begin{bmatrix} w_{12}^* & -w_{11}^* & w_{22}^* & -w_{21}^* \end{bmatrix}^T \tag{A.18}$$

Eq.A.17 and A.18 become the pattern of weight vectors.

Bibliography

[1] J. B. Anderson, "Array Gain and Capacity for Known Random Channels with Multiple Element Arrays at Both Ends", *IEEE J. Sel. Areas Commun.,* vol.18, no. 11, pp.2172-2178, November 2000.

[2] B. Hassibi and B. M.Hochwald, "How Much Training is Needed in Multiple-Antenna Wireless Link?," *IEEE Trans. Inf. Theory,* vol.49, No.4, April 2003.

[3] J.K. Cavers, "An Analysis of Pilot Symbol Assisted Modulation for Rayleigh Fading Channels," *IEEE Trans. Veh. Technol.*, vol.40, pp. 686-693, Nov.1991.

[4] J.K. Cavers and J. Varaldi, "Cochannel Interference and Pilot Symbol Assisted Modulation,"*IEEE Trans. Veh. Technol.*, vol.42, pp. 407-413, Nov.1993.

[5] J.K. Cavers, "Pilot Symbol Assisted Moduation and Differentail Detection in Fading and Delay spread" *IEEE Trans. Commun.*, vol.43, pp. 2206-2212, July.1995.

[6] S. Sampei and T. Sunaga, "Rayleigh Fading Compensation for QAM in Land Mobile Radio Communicatins" *IEEE Trans. Veh. Technol.*, vol.42, pp. 137-147, May.1993.

[7] W.Y. Kuo and M.P. Fitz, "Frequency Offset Compensation of Pilot Symbol Assisted Modulation in Frequency Flat Fading," *IEEE Trans. Commun.*, vol.45, pp. 1412-1416, Nov.1997.

[8] M.K. Tsatsanis and Z. Xu "Pilot Symbol Assisted Modulation in Frequency Selective Fading Wireless Channels," *IEEE Trans. Signal process.*, vol.48, pp. 2353-2365, Aug.2000.

[9] Y. Chen and N.C. Beaulieu, "Optimum Pilot Symbol Assisted Modulation," *IEEE Trans. Commun.*, vol.55, pp. 1536-1546, Aug.2007.

[10] J.C. Guey, M. P. Fitz, M.R. Bell, and W.Y. Kuo, "Signal design for transmitter diversity wireless communication systems over Rayleigh fading channels," *IEEE Trans. Commun.*, vol. 47, pp. 527-537, April 1999.

[11] C. Cozzo and B.L. Hughes, "Joint Channel Estimation and Data Detection in Space-Time Communications," *IEEE Trans. Commun.*, vol.51, pp.1266-1270, August 2003.

[12] J. Kim and Y.S. Cho, "A Comparison of Orthogonal Space-Time Block Codes for Fast Fading," *IEICE Trans. Commun.*, vol.E88-B, no.7, pp.3069-3072, July 2005.

[13] D.V. Duong and G.E. Oien, "Optimal Pilot Spacing and Power in Rate-Adaptive MIMO Diversity Systems with Imperfect CSI," *IEEE Trans. Wireless Commun.,* vol.6, pp.845-851, Mar. 2007.

[14] H. P. Bui, Y. Ogawa, T. Ohgane and Toshihiko Nishimura, "Channel Extrapolation Techniques for E-SDM System in Time-Varying Fading Environments,"*IEICE Trans. Commun.,* vol.E89-B, no.11, November 2006.

[15] S. M. Alamouti, "A Simple Transmit Diversity Technique for Wireless Communications," *IEEE J. Sel. Areas Commun.*, vol. 16, no. 8, pp. 1451-1458, Oct. 1998.

[16] V. Tarokh, H. Jafarkhani, and A. R. Calderbank, "Space-Time Block Codes from Orthogonal Designs," *IEEE Trans. Inf. Theory*, vol.45, no.5, pp. 1456-1467, July 1999.

[17] V. Tarokh, N. Seshadri, and A.R. Calderbank, "Space-Time Codes for High Data Rates Wireless Communications: Performance Analysis and Code Construction," *IEEE Trans. Inf. Theory*, vol. 44, no. 2, pp. 744-765, Mar. 1998.

[18] V. Tarokh, H. Jafarkhani, and A.R. Calderbank, "Space-Time Block Coding for Wireless Communications: Performance Results," *IEEE J. Sel. Areas Commun.*, vol. 17, no. 3, pp. 451-460, Mar. 1999.

[19] V. Tarokh, A. Naguib, N. Seshadri, and A.R. Calderbank, "Space-Time Codes for High Data Rate Wireless Communication: Performance Criteria in the Presence of Channel Estimation Errors, Mobility, and Multiple Paths," *IEEE Trans. Commun.*, vol. 47, no. 2, pp. 199-207, Feb. 1999.

[20] A. Wittneben, "A New Bandwidth Efficient Transmit Antenna Modulation Diversity Scheme for Linear Digital Modulation," *Proc.1993 IEEE International Conf. Commun. (ICC'93)*, 1993.

[21] N. Seshadri and J. H. Winters, "Two Signaling Schemes for Improving the Error Performance of Frequency-Division-Duplex (FDD) Transmission System," *International Journal of Wireless Information Networks, Springer*, vol. 1, no. 1, pp. 1068-9605, Jan. 1994.

[22] S. Sandhu, R. Heath, and A. Paulraj, "Space-Time Block Codes Versus Space-Time Trellis Codes," *Proc.2001 IEEE International Conf. Commun. (ICC'01)*, Helsinki, Finland, vol. 4, pp. 1132-1136, June 2001.

[23] A. Wittneben, "Base Station Modulation Diversity for Digial SIMULCAST," in *Proc.1991 IEEE Vehicular Technology Conf. (VTC 41st)*, pp. 848-853, May 1991.

[24] J. H. Winters, "The Diversity Gain of Transmit Diversity in Wireless Systems with Rayleigh Fading,"*IEEE Trans. Veh. Technol.*, vol.47, No.1, pp.119-123, February 1998.

[25] V. Tarokh and H. Jafarkhani, "A Differential Detection Scheme for Transmit Diversity," *IEEE J. Sel. Areas Commun.*, vol.18, pp.1169-1174, July 2000.

[26] C. Ling, K. H. Li, Alex C. Kot, and Q.T. Zhang, “Multisampling Decision-Feedback Linear Prediction Receivers for Differnetial Space-Time Modulation over Rayleigh Fast-Fading Channels,” *IEEE Trans. Commun.*, vol.51, pp.1214-1223, July 2003.

[27] E. Chiavaccini and G. M. Vitetta, “Further Results on Differential Space-Time Modulations,” *IEEE Trans. Commun.*, vol.51, pp.1093-1101, July 2003.

[28] J. Hou and M. H. Lee, “QPSK Differential Space-Time Coding on Different Unitary Matrices Sets and Initialization,” *IEICE Trans. Fundamentals*, vol.E89-A, pp.348-353, January 2006.

[29] Y. Li and B. Vucetic, “Design of Differential Space-Time Trellis Codes,” *IEEE Trans. Wireless Commun.*, vol.6, pp.1631-1637, May 2007.

[30] P.K. Bondyopadhyay, “The First Application of Array Antenna” *Proc.2000 IEEE Phased Array Systems and Technology,* Texas, USA, 2000, pp.29-32, 2000.

[31] S. Andersson, B. Carlqvist, B. Hagerman, and R. Lagerholm, “Enhancing Cellular Network Capacity with Adaptive Antennas,” *Ericsson Review,* vol.76, pp.138-141, no.3, 1999.

[32] H. Dam, M. Berg, S. Andersson, R. Bornmann, M. Frerice, and T. Hen,“Performance Evaluation of Adaptive Antenna Base Stations in a Commercial GSM Network,” *Proc.1999 IEEE Vehicular Technology Conf.(VTC50th),* Piscataway, USA, pp.47-51, 1999.

[33] K. Sheikh, D. Gesbert, D. Gore, and A.J. Paulraj, “Smart Antennas for Broadband Wireless Access Networks,” *IEEE Signal Processing Magazine,* vol.37, no.11, pp.100-105, Nov.1999.

[34] R.T. Derryberry, S.D. Gray, D.M. Ionescu, G. Mandyam, and B. Raghotaman, “Transmit Diversity in 3G CDMA Systems,” *IEEE Commun. Magazine,* vol.40, no.4, pp.68-75, April 2002.

[35] S. Andersson and B. Hagerman, “Adaptive Antennas in Wireless Systems Basics Background and Field-Trial Results,” *Proc.1999 Radiovetenskaplig Konferens*, Karskrona, Sweden, pp.249-253, 1999.

[36] S. Andersson, U. Forssen, J. Karlsson, T. Witsschel, P. Fischer, and A. Krug, “Ericsson/Mannesmann GSM Field Trials with Adaptive Antennas,” *Proc.1997 IEEE Vehicular Technology Conf. (VTC47th),* Phoenix, USA, pp.1587-1591, May 1997.

[37] J. Strandell, M. Wennstrom, A. Rydberg, T. Oberg, O. Gladh, L. Rexberg, E. Sandberg, B.V. Andersson, and M. Appelgren, “Experimetal Evaluation of An Adaptive Antenna for a TDMA Telephony System,” *Proc.1997 IEEE Personal Indoor and Mobile Radio Communications Conf. (PIMRC10th),* Helsinki, Finland, pp. 79-84, Sept.1997.

[38] J. Strandell, M. Wennstrom, T. Oberg, and A. Rydberg,“Design and Evaluation of A Fully Adaptive Antenna for Telecommunication Systems,” *Proc.1997 Antenna Conf.*, Gothenburg, Sweden, pp.357-366, 1997.

[39] S.M. Simmonds and M. Beach,“Downlink Calibration Requirements for the TSUNAMI(II) Adaptive Antenna Testbed,” *Proc.1998 The ninth Personal, Indoor and Mobile Radio Communications,* Boston, USA, 8-11 September 1998.

[40] P.E. Mogensen,K.I. Pedersen,P. Leth-Espensen, B. Fleury, F. Fredriksen, and K. Olesen, “Preliminary results from an adaptive antenna array tested for GSM/UMTS,” *Proc.1997 IEEE Vehicular Technology Conf.(VTC47th),Phoenix, USA*, pp.1592-1596, May 1997.

[41] G. Tsoulos, M. Beach, and J. McGeehan, “Space Division Multiple Access (SDMA) Field Trials. Part2:Calibration and Linearity Issues,” *Proc.1998 IEE Radar, Sonar and Navigation*, vol.145, no.1, pp.79-84, Feb.1998.

[42] X. N. Tran, T. Taniguchi and Y. Karasawa, “Spatio-Temporal Equalization for Space-time Block Coded Transmission over Frequency Selective Fading Channel with Co-channel Interference”, *IEICE Trans. Fundamentals*, vol. E88-A, no.3, pp.660-668, March. 2005.

[43] T.S. Rappaport, *Wireless Communications-Principles and practice*, 2nd ed., Prentice-Hall, Englewood Cliffs, NJ, 2001.

[44] R.H. Clark, “*A statistical theory of mobile radio reception,” Bell System Tech. J.*, pp.957-1000, July/August 1968.

[45] W.C. Jakes, Jr., *Microwave Moile Communications,* Wiley, New York, 1974.

[46] G.J. Foschini, “Layered Space-Time Architecture for Wireless Communication in a Fading Environment when Using Multi-Element Antennas,” *Bell Labs Technical Journal*, Autumn 1996.

[47] A.J. Paulraj and C.B Papadius, “Space-Time Processing for Wireless Communications,” *IEEE Signal Processing. Mag.*, vol.14, no.6, pp.49-83, Nov. 1997.

[48] M. Schwartz, W.R. Bennett, and S. Stein, *Communication Systems and Techniques*, 1st edition, McGraw-Hill, 1966.

[49] T.S. Rappaport, A. Annamalai, R.M. Buehrer, and W.H. Tranter, “Wireless Communications: past present and a future perspective,” *IEEE Trans. Commun.*, vol. 40, no. 5, pp.148-161, May 2002.

[50] G. J. Foschini, Jr. and M. J. Gans, “On Limits of Wireless Communication in a Fading Environment when Using Multiple Antennas,” *Wireless Personal Communications*, vol. 6, pp. 311-335, 1998.

[51] E. Teletar, “Capactiy of Multiantenna Gaussian channels,” AT&T Bell Laboratories, Tech. Memo., June 1995.

[52] E. Teletar, “Capacity of Multiantenna Gaussian channels,” *Eur. Trans. Commun.,* vol. 10, no. 6, pp.585-595, 1999.

[53] D. Shiu, *Wireless Communication Using Dual Antenna Arrays,* International Series in Engineering and Computer Science. Norwell, MA; Kluwer, 1999.

[54] F.R. Farrokhi, G.J. Foschini, A. Lozano, and R.A. Valenzuela,“Link Optimal Water-Filling in Vector Multiple-Access Channels” *IEEE Commun. Lett.,* vol.5, pp.85-87, 2001.

[55] C.N. Chuah, D.N.C. Tse, and V. Anantharam,“Asymptotically Optimal Water-Filling in Vector Multiple-Access Channels, ” *IEEE Trans. Inf. Theory,* vol.47, pp.637-650, Mar.2002.

[56] G. J. Foschini, Jr. and M. J. Gans, “On Limits of Wireless Communication in a Fading Environment when Using Multiple Antennas,” *Wireless Personal Communications*, vol. 6, pp. 311-335, 1998.

[57] P. W. Wolniansky, G.J. Foschini, G. D. Golden, and R. A. Valenzuela, “V-BLAST: An Architecture for Realizing Very High Data Rates over The Rich-Scattering Wireless Channel, *Proc.1998 IEEE-URSI Signals, Systems, and Electronics*, pp. 295-300, Oct. 1998.

[58] R. T. Compton, “The Relationship Between Tapped Delay Line and FFT Processing in Adaptive Arrays,” *IEEE Trans. Antennas Propagat.*, vol.36, no.1, pp.15-26, Jan. 1988.

[59] B. Widrow, P. E. Mantey, L.J. Griffiths, and B. B. Goode, “Adaptive Antenna System,” *Proc.1967 IEEE*, vol. 55, no. 12, pp. 2143-2159, Dec. 1967.

[60] N. Kikuma, *Adaptive Antenna Technology* (in Japanese), Ohmsha, Ltd., Oct. 2003.

[61] G. V. Tsoulos, “Smart Antennas for Mobile Communication Systems: Benefits and Challenges,” *Electronic and Communication Engineering Journal*, vol. 11, no. 2, pp. 84-94, Apr. 1999.

[62] R. A. Monzingo and T. W. Miller, *Introduction to Adaptive Arrays*, John Wiley & Sons, 1980.

[63] J. E. Hudson, *Adaptive Array Principles*, The Institution of Engineering and Technology, 1991.

[64] S. C. Swales, M. A. Beach, and D. J. Edwards, “Multi-Beam Adaptive Base Station Antennas for Cellular Land Mobile Radio Systems,” *Proc.1989 IEEE Vehicular Technology Conf.(VTC39th)*, vol. 1, pp. 341-348, 1989.

[65] S. C. Swales, M. A. Beach, D. J. Edwards, and J. P. McGeehan, “The Performance Enhancement of Multibeam Adaptive Base-Station Antennas for Cellular Land Mobile Radio Systems” *IEEE Trans. Veh. Technol.*, vol.39, pp.56 - 67, Feb 1990.

[66] J. Litva, Titus Kwok-Yeung Lo., *Digital Beamforming in Wireless Communications*, Norwood MA: Artech House, 1996.

[67] J. D. Parson, *The Mobile Radio Propagation Channel*, London: Pentech House 1992.

[68] S. R. Saunders, *Antennas And Propagation For Wireless Communication Systems*, New York: John Wiley and Sons, 1999.

[69] S. Annanab, T. Taniguchi and Y. Karasawa "MIMO STBC Adaptive Array for Fast Fading Channel", *IEICE Trans. Commun.*, vol. E90-B no.9, pp.2321-2329, Sept. 2007.

List of Original Publication Related to the Thesis

Journals

1. S.Annanab, T. Taniguchi, and Y. Karasawa, "MIMO STBC Adaptive Array for Fast Fading Channel," *IEICE Trans. Communs.*, vol.E90-B, no.9, pp.2321-2329, 2007.

2. S.Annanab, T. Tobita, T. Taniguchi, and Y. Karasawa, "Asynchronous MIMO STBC Adaptive Array Transmission System for Multiuser over Fast Fading Channel," *IEICE Trans. Communs.*, vol.E91-B, no.08, pp.2666-2673, 2008..

International Conferences

1. S. Annanab, T. Tobita, T. Taniguchi, and Y. Karasawa, "Multiuser Asynchronous MIMO STBC Adaptive Array Transmission Scheme in Fast Fading Channel," 2008 IEEE 68th Vehicular Technology Conference(VTC2008-Fall), Calgary, Canada, Sept.21-24, 2008.

2. S. Annanab, T. Taniguchi, and Y. Karasawa, "Multiuser Asynchronous Transmission System with MIMO STBC Adaptive Array over Fast Fading Channel," International Symposium on Advanced ICT(AICT2007), BUPT, Beijing, China, Sept. 2007.

3. S. Annanab, T. Taniguchi, and Y. Karasawa, "Adaptive Beamforming for MIMO STBC over Fast Fading Channel," 2006 International Symposium on Antenna and Propagation (ISAP'06), Singapore, Nov. 1-4, 2006.

4. S. Annanab, T. Taniguchi, and Y. Karasawa, "MIMO STBC Data Transmission Scheme for Inter-Vehicle Communications at 60 GHz in ITS," 2004 International Symposium on Antenna and Propagation (ISAP'04), Sendai, Japan , Aug. 17-21, 2004.

Oral Presentations

1. S. Annanab, T. Tobita, T. Taniguchi, and Y. Karasawa, "Asynchronous MIMO STBC Adaptive Array Transmission Scheme for Multiuser over Fast Fading Channel," IEICE Society Conference, B-1-231, Mar, 2008.

2. S. Annanab, T. Tobita, T. Taniguchi, and Y. Karasawa, "MIMO STBC Adaptive Array for Fast Fading Channel" IEICE Technical Report AP2007-143, pp.231-236, Jan. 2008.

3. S. Annanab, T. Taniguchi, and Y. Karasawa, "MIMO STBC Adaptive Array for Fast Fading Channel," IEICE Technical Report AP2006-83, pp.41-46, Oct. 2006.

4. S. Annanab, T. Taniguchi, and Y. Karasawa, "MIMO STBC Adaptive Array in Fast Fading Environment," IEICE Society Conference, B-1-210, Sept., 2006.

Author Biography

Supawan Annanab was born in Nonthaburi, Thailand in 1978. She received her B.Eng(Electrical Engineering) from Kasetsart University, Thailand in 2000 and M.Eng(Information Engineering) from King Mongut's Institute of Technology, Ladkrabang(KMITL) Thailand in 2004. During her Master program(2003-2004), she received scholarship from Association of International Education, Japan (AIEJ) as an exchange student in the University of Electro-Communications where she had the opportunity to study in Karasawa Laboratory. After 6 months of her exchange program finished, she entered to continue higher education as a Ph.D. student in the same laboratory in the University of Electro-Communications, Japan. Her research interests are in the area of space-time processing, MIMO, ITS(Intelligent Transport System), and adaptive array antenna.

She is a student member of the Institute of Electronics, Information and Communications Engineer(IEICE), Japan and the Institute of Electrical Engineering (IEEE).